[Cell Cycle 8:17, 2794-2801; 1 September 2009]; ©2009 Landes Bioscience

Report

Common light signaling pathways controlling DNA repair and circadian clock entrainment in zebrafish

Jun Hirayama,[1,†,*] Norio Miyamura,[2,†] Yoshimi Uchida,[2] Yoichi Asaoka,[2] Reiko Honda,[1] Kenji Sawanobori,[2,3] Takeshi Todo,[4] Takuro Yamamoto,[5] Paolo Sassone-Corsi[6,*] and Hiroshi Nishina[2]

[1]Medical Top Track Program; and [2]Department of Developmental and Regenerative Biology; Medical Research Institute; Tokyo Medical and Dental University; Bunkyo-ku, Tokyo Japan; [3]Department of Physiological Chemistry; Graduate School of Pharmaceutical Sciences; University of Tokyo; [4]Department of Radiation Biology and Medical Genetics; Graduate School of Medicine; Osaka University; Suita, Osaka Japan; [5]Life Science Laboratory; Advanced Materials Laboratories; Sony Corporation; Bunkyo-ku, Tokyo Japan; [6]Department of Pharmacology; University of California; Irvine, CA USA

†These authors contributed equally to this work.

Abbreviations: PHR, photolyase; CRY, cryptochrome; redox, reduction/oxidation; MAPK, mitogen-activated protein kinase; ERK, extracellular signal-regulated kinase

Key words: photolyase, cryptochrome, DNA repair, circadian clock, ERK/MAPK signaling

UV radiation causes a number of harmful events including growth delay, cell death and ultimately cancer. The reversal of such effects by concomitant exposure to visible light is a conserved mechanism which has been uncovered in many multi-cellular organisms. Here we show that light-dependent UV-tolerance is a cell autonomous phenomenon in zebrafish. In addition, we provide several lines of evidence indicating that light induction of 64PHR, a DNA repair enzyme, and the subsequent light-dependent DNA repair mediated by this enzyme are prerequisites for light-mediated UV tolerance. 64PHR is evolutionary related to and has a high degree of structural similarity to animal CRY, an essential circadian regulator. The zebrafish circadian clock is controlled by a cell-autonomous and light-dependent oscillator, where zCRY1a functions as an important mediator of light entrainment of the circadian clock. In this study, we show that light directly activates MAPK signaling cascades in zebrafish cells and we provide evidence that light-induced activation of these pathways controls the expression of two evolutionary-related genes, *z64Phr* and *zCry1a*, revealing that light-dependent DNA repair and the entrainment of circadian clock share common regulatory pathways.

*Correspondence to: Jun Hirayama; Medical Top Track Program; Medical Research Institute; Tokyo Medical and Dental University; 1-5-45 Yushima; Bukyo-ku; Tokyo, Japan; Tel.: 81.3.5803.4658; Fax: 81.3.5803.5829; Email: hirayama.mtt@mri.tmd.ac.jp / Paolo Sassone-Corsi; Department of Pharmacology; University of California at Irvine; 92697 CA; Tel.: 949.824.4540; Fax: 949.824.2078; Email: psc@uci.edu

Submitted: 06/24/09; Accepted: 07/06/09

Previously published online as a *Cell Cycle* E-publication: http://www.landesbioscience.com/journals/cc/article/9447

Introduction

Sunlight is essential for life on Earth and organisms have evolved various methods for the efficient utilization of this source of energy. The UV component of sunlight, however, threatens life by producing cytotoxic, mutagenic and carcinogenic lesions within DNA.[1,2] The main UV radiation-induced lesion is the pyrimidine dimer produced at a di-pyrimidine site on DNA. Therefore nature exerted a selective pressure to develop a self-defense system such as the one mediated by DNA photolyases (PHRs).[3,4] The DNA PHRs repair UV-induced pyrimidine dimers by utilizing light of the near-UV/blue-light region.[5] Two types of PHRs have been described: the cyclobutane pyrimidine dimer (CPD) PHR and the (6-4) pyrimidine-pyrimidone dimer (64)PHR. CPD PHRs have been found in a wide range of organisms, including eubacteria, archaebacteria, plants, insects and vertebrates, whereas the 64PHRs have only been found in some higher eukaryotes including zebrafish.[6] Both the CPD PHRs and 64PHRs belong to the DNA photolyase/cryptochrome protein family which comprises functionally diverse members such as DNA PHR and CRY.[6,7] It has been reported that 64PHR evolved from the animal CRY,[6,8,9] possibly revealing an evolutionary link between DNA repair processes and the circadian clock.

Circadian clocks exist in a variety of organisms ranging from bacteria to humans and regulate various biochemical, physiological and behavioral processes.[10,11] Under natural conditions, rhythms are entrained to a 24-h cycle by environmental time cues, in which light being the most important. The core of the circadian clock mechanism is a cell-autonomous and self-sustained oscillator based on a transcription/translation-based negative-feedback loop that relies on positive and negative oscillator elements.[12] In vertebrates, two basic helix-loop-helix PAS (PER-ARNT-SIM) domain-containing transcription factors, CLOCK and BMAL1,

constitute the positive elements. Upon heterodimerization, CLOCK:BMAL1 drives the transcription of the negative components of the clock machinery, *Cryptochrome* (*Cry*) and *Period* (*Per*) genes. CRY and PER negatively regulate their own expression, setting up the rhythmic oscillations of gene expression that drive the circadian clock.[13,14]

Zebrafish has been established as an attractive vertebrate cell-based model suitable to study the light signaling pathway and its impact on the circadian clock.[15] Zebrafish possess an intrinsic autonomous oscillator that consists of components similar to those of mammals.[16] In addition, zebrafish oscillators in peripheral tissues, as well as in cultured cell lines derived from them, display direct-light responsiveness.[17,18] In zebrafish cells, light directly activates the expression of a specific *Cry* gene, *zCry1a*. Light-induced zCRY1a functions as an essential transcriptional repressor to mediate the light-dependent entrainment of the circadian clock.[19,20]

The reduction of lethal and mutagenic effects of UV radiation by visible light exposure, a phenomenon known as light-induced UV-tolerance, has been identified in a variety of organisms including the zebrafish embryo.[21-23] In this study, we show that the light-induced UV tolerance in zebrafish is a cell autonomous phenomenon. We also provide several lines of evidence indicating that both the light induction of 64PHR and the subsequent light-dependent DNA repair by 64PHR are essential for light-induced UV tolerance. Finally, we found that light-induced activation of MAPK signaling pathways controls the expression of two evolutionary-related genes, *z64Phr* and *zCry1a*, revealing that light-dependent UV-tolerance and entrainment of the circadian clock are part of a common light-regulatory cascade.

Results

Light improves survival of zebrafish cultured cell. There is evidence indicating that visible light increases the survival of UV-irradiated bacteria.[21,22] Importantly, the same phenomenon has been also reported in a variety of higher organisms.[23,24] In order to test if visible light-induced UV tolerance is a cell autonomous effect in multi-cellular organisms, we first examined the effects of different lighting regimes (DD, LD, DL and LL) on the survival of UV light-irradiated zebrafish cultured cells (Fig. 1A and B). We have chosen zebrafish as a model system because its peripheral tissues and derived cultured cell lines contain cell-autonomous circadian oscillators, which respond directly to visible light.[17,18] In untreated controls, there were no significant differences in the survival of cells cultured in each lighting condition (Fig. 1A upper and B, lanes 1, 3, 5 and 7), indicating that visible light is not harmful to zebrafish cells. When cells were exposed to visible light after UV irradiation, they had a survival level slightly higher than that of cells without visible light treatment or cells treated with visible light before UV irradiation (Fig. 1A panels 1–3, B lanes 2, 4 and 6). This light-dependent survival improvement became much more evident when cells were exposed to visible light both before and after UV irradiation (Fig. 1A panel 4, and B lane 8). These results show that the visible light-induced UV tolerance is cell autonomous in zebrafish and furthermore, that visible light treatment both before and after UV irradiation is necessary for the cell to acquire UV-tolerance.

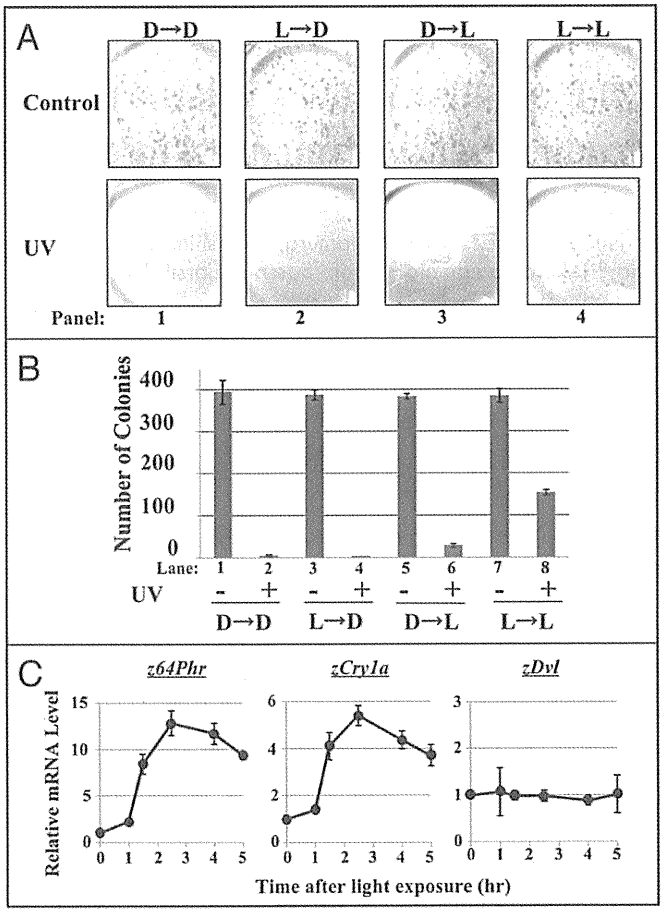

Figure 1. Effect of different lighting regimes on the survival of UV-irradiated zebrafish cultured cells. (A) Representative colonies of zebrafish cultured cells treated with (UV) or without (control) 20 J/m^2 of UV light. Four different lighting regimes were applied to the cells. (1) Cells were kept in dark before and after UV irradiation (DD). (2) Cells were exposed to visible light for 3.5 hrs before UV irradiation and kept in the dark after UV irradiation (LD). (3) Cells were kept in the dark before UV irradiation and exposed to visible light for 1.5 hrs after UV irradiation (DL). (4) Cells were exposed to visible light for 3.5 hrs and 1.5 hrs before and after UV irradiation, respectively (LL). (B) The number of surviving colonies described in (A) was counted. Each value is the mean ± SEM of three independent experiments. (C) Zebrafish cultured cells maintained in constant darkness were exposed to light, and RNA was harvested at each time point indicated after light onset. *z64Phr*, *zCry1a* and *zDvl* gene expression was examined by RT-qPCR analysis and normalized against zebrafish actin gene. The value from the cells kept in the dark was set as 1 for each gene. Each value is the mean ± SEM of three independent experiments. In this experiments, we used the cells infected with the empty pCLNCX retrovirus vector (Fig. 2A). We have confirmed that retrovirus infection itself has no effect on the cell survival and gene expression.[20,35] (data not shown).

Light induces *z64phr*, a DNA repair enzyme. We next sought to identify the factor involved in the visible light-induced UV-tolerance in zebrafish cultured cells. We therefore decided to screen by quan-

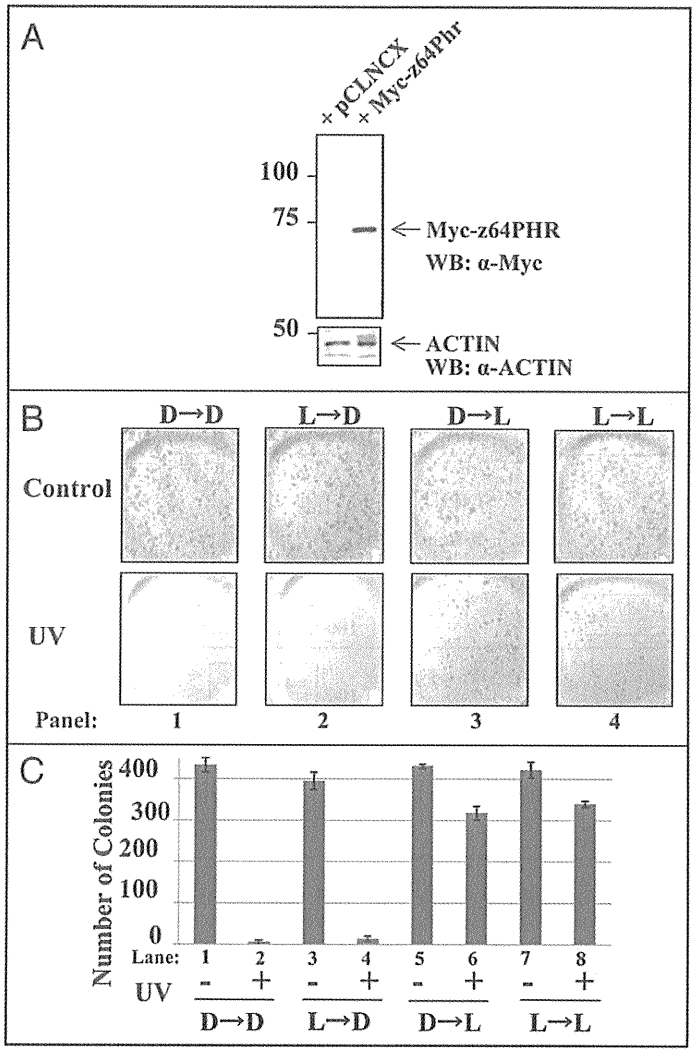

Figure 2. Light-dependent DNA repair mediated by z64PHR is an essential element of the light-induced UV-tolerance in zebrafish cells. (A) Expression of retrovirally-infected Myc-z64PHR in zebrafish cultured cells was confirmed by western blotting (WB) with Myc antibody (upper). The same cell lysates were immunoblotted with an antibody against actin as a loading control (lower). (B) Representative colonies of the ectopically 64PHR-expressing cells treated with (UV) or without (control) 20 J/m^2 UV. The same four lighting regimes described in Figure 1 were applied to the cells. (C) The number of surviving colonies was counted. Each value is the mean ± SEM of three independent experiments.

titative PCR and western analysis the light-dependent expression profile of various factors involved in different cellular functions including Wnt signaling pathway, MAPK signaling pathway, the circadian clock, DNA repair, the cell cycle and the cellular redox (reduction/oxidation) state. The results from representative factors analyzed are summarized in Supplemental Table. The effects of 5 hr light exposure were categorized as upregulated, no change (NC), and downregulated. Among all factors analyzed, the expression of 64 photolyase (*64phr*) gene showed a remarkable light-dependent induction. 64PHR is a DNA repair enzyme that repairs the DNA lesion by utilizing visible light energy.[25,26] Interestingly, it is important to stress again its evolutionary and structural relation to CRY, an essential circadian clock protein.[5,6] (Suppl. Fig. 1).

To better understand how light regulates *z64Phr,* we decided to perform a kinetic analysis to examine the effect of light on *z64Phr* gene expression. The zebrafish cultured cells were kept in constant darkness for 3 days and then exposed to light. In agreement with our previous observation, *z64Phr* expression was strongly induced by light (Fig. 1C). Interestingly the light-dependent expression pattern of *z64Phr* is reminiscent of *zCry1a* expression we have previously reported.[20,27] We next evaluated the kinetics of light induction of *zCry1a* and found that *zCry1a* induction displays a similar kinetics than that of *z64Phr* (Fig. 1C), suggesting that a common signaling pathway could be responsible for the light induction of both *z64Phr* and *zCry1a* genes. Knowing that 64PHR repairs DNA lesion by utilizing visible light energy,[26] the light-dependent induction of *z64phr* strongly indicates that visible light treatment before UV irradiation is required for z64PHR accumulation in cells.

z64PHR is responsible for light-induced UV-tolerance. Having established that zebrafish cells need to be treated with visible light before and after UV exposure to obtain UV-tolerance (Fig. 1A and B), we then speculated that visible light treatment after UV irradiation would be required as energy for the light-dependent repair mediated by 64PHR. To test this hypothesis, we infected zebrafish cultured cells with retroviral vectors to induce the ectopic expression of the *z64Phr* (pCLNCX-*z64Phr*) gene (Fig. 2A) and assessed the effect of light on the survival of the infected cells.

Cells were treated with the above-mentioned four lighting regimes (DD, LD, DL and LL) (Fig. 1). In untreated controls, the ectopic expression of z64PHR had no effect on the survival of cells independent of the lighting condition (Compare Figs. 1B lanes 1, 3, 5, 7 and 2C lanes 1, 3, 5, 7). However, the ectopic expression of z64PHR improved the survival of cells treated with visible light both before and after UV irradiation (Compare Figs. 1B lanes 8 and 2C), providing evidence that z64PHR plays a role in the light-induced UV tolerance. Importantly, cells expressing ectopic z64PHR became UV-tolerant when they were treated with visible light after UV exposure. This acquisition of UV-tolerance was not dependent on the lighting condition prior to UV exposure (Fig. 2B panels 3 and 4, and C lanes 6, 8). These results are consistent with the notion that visible light treatment before UV irradiation is required for the accumulation of z64PHR in the cell. Finally, visible light treatment after UV irradiation was necessary to increase survival rates (Fig. 2B panels 1, 2, and C lanes 2, 4). This observation could reflect the fact that visible light treatment after UV irradiation is essential to provide an energy source for the light-dependent DNA repair mediated

by 64PHR, further supporting the idea that z64PHR is involved in the light-induced UV tolerance.

z64PHR is not involved in circadian regulation. Light directly entrains circadian transcription in zebrafish cells.[17,18] In fact, visible light treatment which renders the cell UV-tolerant (Fig. 1) can concomitantly induce circadian entrainment (Fig. 3A). In addition, z64PHR and zCRY1a are both members of the DNA photolyase/cryptochrome family and share significant high structural homology.[5,6] (Suppl. Fig. 1) Given that zCRY1a plays a role in light entrainment of the circadian clock[19,20] and the light induction kinetics of *z64Phr* and *zCry1a* are similar (Fig. 1C), we decided to test if light-induced z64PHR participates in the circadian oscillator. We first analyzed the expression of a clock-controlled gene, *Per1*, in zebrafish cultured cells overexpressing z64PHR. In contrast to the previously reported repression of *Per1* rhythmic expression by zCRY1a,[19] overexpression of z64PHR did not alter the circadian expression of *Per1* (Fig. 3A). In the circadian feedback loop, the CLOCK:BMAL1 heterodimer functions as the transcriptional activator[10,28] and the inhibition of CLOCK:BMAL1-mediated transcription is an essential element for the light-dependent entrainment of the zebrafish circadian clock.[19,20] We therefore decided to study the effect of z64PHR on CLOCK:BMAL1-mediated transcription by means of a luciferase reporter gene assay (Fig. 3B). Co-expression of CLOCK with BMAL1 strongly stimulated transcription from their target promoter. Overexpression of z64PHR did not affect CLOCK:BMAL1-mediated transactivation whereas zCRY1a efficiently inhibited it. Finally, we examined if z64PHR interacts with CLOCK1:BMAL1 heterodimer and/or PER2, another circadian regulator,[29] by co-immunoprecipitation experiments. Importantly, z64PHR did not interact either with CLOCK1:BMAL1 heterodimer or with PER2, whereas zCRY1a did interact with both (Fig. 3C). Taken together, these results demonstrate that z64PHR is not involved in the transcriptional regulation of circadian clock.

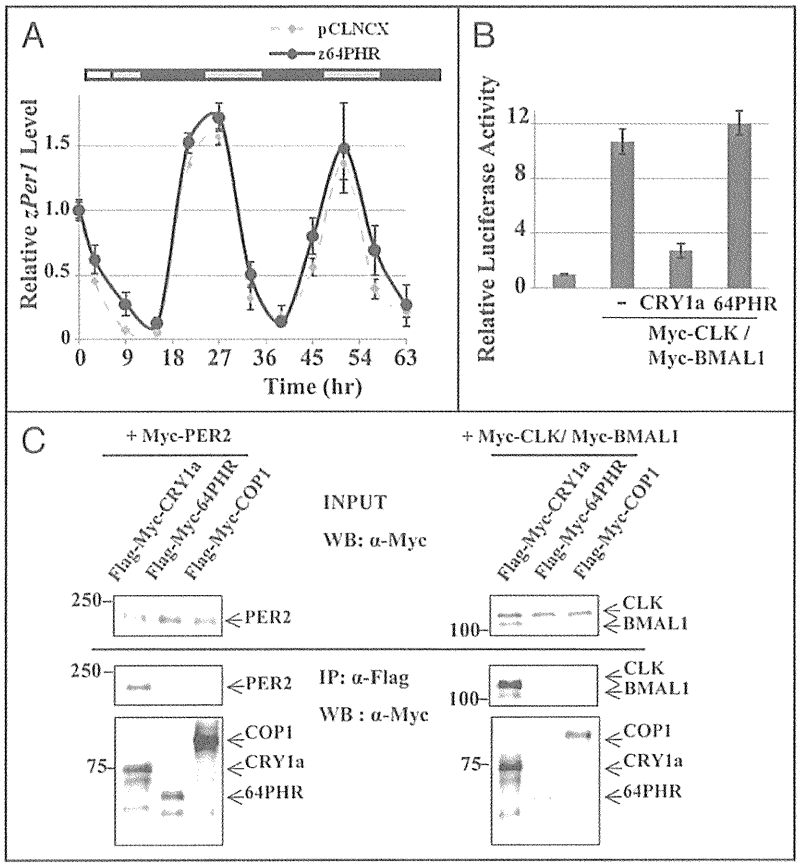

Figure 3. z64PHR is not involved in circadian clock regulation. (A) Oscillation of *zPer1* gene. Cells maintained in constant darkness were exposed to light for 5 hours and then transferred to constant darkness. RNA was harvested at each time point indicated after light onset. *Per1* gene expression was examined by RT-qPCR analysis. The value from the cells at time point 0 was set as 1. Each value is the mean ± SEM of three independent experiments. The bar above the blots indicates light (white), subjective day (grey), and subjective night (black) periods. (B) The effects of 64PHR and CRY1a proteins on CLOCK:BMAL-mediated transcription were examined by a luciferase reporter gene assay in cultured cells. CLOCK and BMAL were co-expressed with 64PHR or CRY1a, and the effects on transcriptional activation of the reporter plasmid were assayed. The relative luciferase activities (means ± the standard deviations; $n = 3$) are presented. (C) Flag-Myc-CRY1a or Flag-Myc-64PHR was co-expressed with Myc-CLOCK and Myc-BMAL (right) or with Myc-PER2 (left) in cultured cells. The cell lysates were immunoprecipitated (IP) with the Flag antibody. Immunoprecipitated material was analyzed by western blotting (WB) with Myc antibody. Analyses of total cell lysate with Myc antibody confirmed the expression of the three proteins, Myc-CLOCK, Myc-BMAL and Myc-PER2 (top). Constitutive photomorphogenic-1 (COP1) protein was used as negative control of the experiment.

MAP kinase pathways regulate the light-dependent expression of *z64Phr*. We then sought to identify the intracellular signaling pathways responsible for the light-dependent induction of the *z64Phr* gene. In our previous study we demonstrated that light-induced *zCry1a* expression in zebrafish cultured cells is mediated by the activation of the extracellular signal-regulated kinase (ERK) pathway.[20,30] This fact, together with a common expression profile after light induction of *z64Phr* and *zCry1a* genes (Fig. 1C), raises the possibility that MAPK pathways could be involved in the light-dependent *z64Phr* expression. We first analyzed the effects of light on the phosphorylation levels of some key players of MAPK signaling pathways (Fig. 4A and B). After 3 days in darkness, zebrafish cultured cells were exposed to light, and cell extracts were prepared from 0 to 180 min after light exposure. The phosphorylation levels of ERK and MEK were significantly increased 10–30 min after light and then decreased. p38 phosphorylation

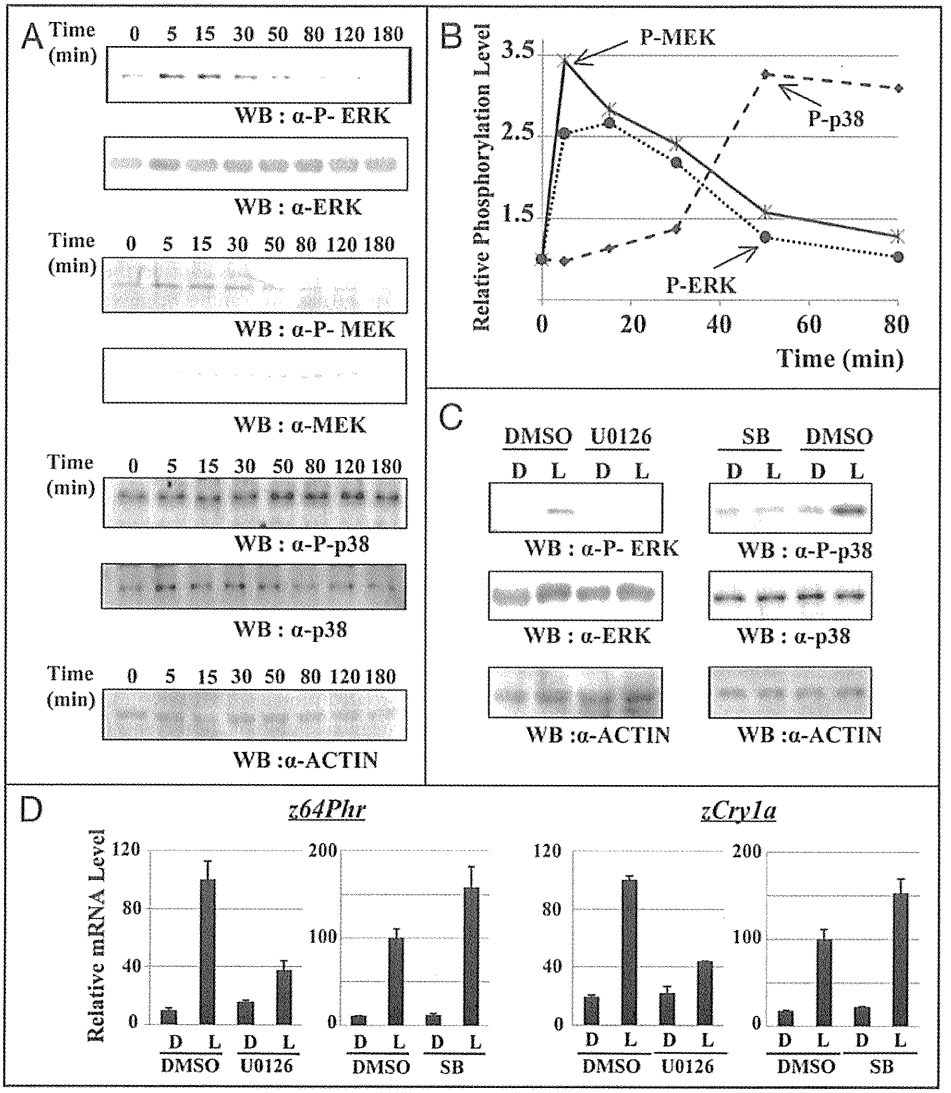

Figure 4. Light directly activates MAPK signaling pathways in zebrafish cultured cell. (A) Kinetics of ERK, MEK and p38 phosphorylation levels induced by visible light in zebrafish cultured cells. The cells permanently cultured in the dark were exposed to visible light. At indicated time points after the light treatment, cells were harvested for western blotting (WB). Similar results were found in replicate experiments. (B) Phospho-ERK, phospho-MEK and phospho-p38 signals obtained in the western blot shown in (A) were quantified and normalized with signals of total ERK, MEK and p38, respectively. The values are expressed as fold stimulation compared with the control levels observed without UV irradiation. (C) Zebrafish cultured cells were treated with U0126 and SB203580 (SB) inhibitors or with the vehicle (DMSO). After 1 h, cells were stimulated with light (L) or were left in the dark (D). For U0126 treatment, cells were harvested 15 min after onset of light. For SB203580 treatment, cells were harvested 90 min after onset of light. The cell extracts were then prepared for western blotting. (D) Effects of U0126 and SB203580 inhibitors on light induction of *z64Phr* and *zCry1a* were tested by RT-qPCR as described in Figure 1C. RNA was prepared 100 min and 180 min after onset of light for U0126 and SB203580 treatments, respectively. The value from the control cells exposed to light was set as 100% for each experiment. Each value is the mean ± SEM of three independent experiments. The concentrations of U0126 and SB203580 inhibitors used were 30 μM and 10 μM, respectively.

levels also increased, but its kinetics was delayed compared to that of ERK and MEK phosphorylation (Fig. 4).

To test if this light-dependent activation of MAPK signaling pathways regulates *z64Phr* transcription, we treated cells with a panel of inhibitors prior to the light pulse (Fig. 4C and D). The MEK-specific inhibitor U0126 drastically blocked *z64Phr* induction, confirming the implication of the ERK pathway in light-induced signaling. We next tested the inhibitor SB203580, specific for the stress-regulated p38 MAPK. This inhibitor potentiated *z64Phr* induction, suggesting that the p38 pathway negatively

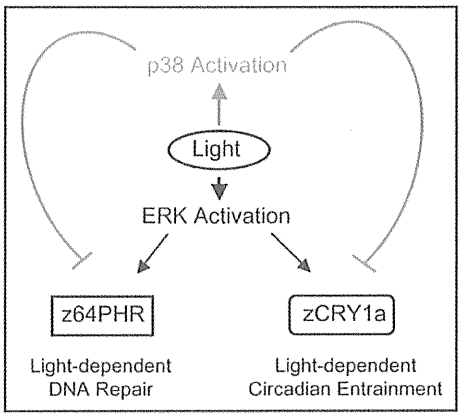

Figure 5. Model depicting the molecular mechanisms underlying light-dependent transcriptional events regulating DNA repair and circadian clock entrainment.

regulates the light-dependent induction of *z64Phr*. Notably, these inhibitors had the same effects on the light-induction of *zCry1a*. These findings provide evidence of a common light signaling pathway regulating both DNA repair process and the circadian clock.

Discussion

In this study, we report that the light-induced UV tolerance in zebrafish is a cell autonomous phenomenon (Fig. 1). Furthermore, our findings demonstrate that visible light renders the cells UV-tolerant by acting on two consecutive steps. First, visible light induces *z64Phr* gene expression thereby increasing 64PHR cellular levels. The induced 64PHR then repairs the DNA lesion by utilizing visible light as source of energy. Both the light induction of 64PHR and the subsequent light-dependent DNA repair by 64PHR are essential for the light-induced UV tolerance, because visible light treatments both before and after UV exposure were required for the cells to become UV-tolerant (Fig. 1). In a previous report, we described that zebrafish 64PHR has a light-dependent DNA repair activity in vitro[8] and we now show that this enzyme has a specific role in the light-induced UV-tolerance response (Fig. 2). Indeed, we propose that the light-dependent DNA repair activity of z64PHR is an essential element of the light-mediated UV-tolerance mechanism of the cell.

Light is essential for life on Earth and organisms have evolved a number of cellular strategies for the efficient utilization of light energy. Interestingly, we found that light directly regulates two important biological events in zebrafish, namely the UV-induced DNA damage tolerance (Fig. 1) and the entrainment of the circadian clock (Fig. 3). Indeed, the light treatment which renders the cell UV-tolerant can also entrain circadian transcription, but our experiments indicate that light-induced z64PHR is not involved in the circadian process (Fig. 3). The zebrafish circadian clock is regulated by a cell-autonomous and self-sustained oscillator, which directly responds to light.[31] This circadian pacemaker is based on a transcription/translation-based negative feedback loop, where zCRY1a functions as an essential transcriptional repressor regulated directly by light to mediate circadian entrainment.[19,31] Importantly, we have previously reported that zCRY1a lacks the light-dependent DNA repair ability.[8] Thus, there is a clear functional divergence between z64PHR and zCRY1a in light-dependent biological events.

Moreover, our results indicate that light directly activates MAPK signaling pathways in a zebrafish cultured cell line (Fig. 4). We also provide evidence that light-induced activation of MAPK signaling pathways controls the expression of both *z64Phr* and *zCry1a* (Fig. 4C and D), revealing that light-dependent DNA repair and entrainment of circadian clock share common regulatory pathways. Importantly, our findings strongly support a possible signaling cross-talk between the ERK/MAPK and p38 pathways for light induction of *z64Phr* and *zCry1a* genes. Indeed, light-activated ERK pathway induces the expression of *z64Phr* and *zCry1a* genes whereas the p38 pathway suppresses it (Fig. 4), showing that ERK/MAPK and p38 pathways oppose each other as a means of regulating light-dependent transcription of *z64Phr* and *zCry1a*. Consistently with our observations, it has been recently reported that the p38 signaling cascade inhibits ERK pathway to induce apoptosis,[32,33] providing further evidence of the signaling cross-talk between the two MAPK signaling pathways.

In summary, we propose a working model in which two evolutionary-related proteins, z64PHR and zCRY1a, play distinct roles in light-regulated physiological events (Fig. 5). Light activates both ERK and p38 MAPK signaling pathways. The former positively regulates expression of both *z64Phr* and *zCry1a* genes whereas the latter negatively controls it. The light-induced z64PHR repairs DNA lesions by utilizing visible light energy (Figs. 1 and 2), thereby rendering the cell UV-tolerant. On the other hand, the light-induced zCRY1a entrains the circadian clock by acting as a transcriptional repressor[19,20] (Fig. 3). Intriguingly, despite their functional diversity, the expression of *z64Phr* and *zCry1a* genes is regulated by the same light signaling cascade, underscoring the functional interplay of *DNA photolyase* and *Cryptochrome* genes through a common transcriptional pathway.

Materials and Methods

Plasmids. Full zebrafish *64Phr* ORF was amplified by PCR with the following primers: 64Phr FW 5'-GCG AAT TCA TGA GCC ATA ACA CCA TTC AC-3' and z64Phr RW 5'-GCC TCG AGT TAT CTC TTT GCC TTC TTC TG-3'. The full length of z64Phr cDNA was cloned in Flag-Myc-pCMV vector. The other plasmids have been described elsewhere.[8,29,34,35]

Cells, transfection and luciferase assay. Zebrafish cultured cells were prepared as described previously.[18,36] They were cultured at 28°C in L-15 medium (Invitrogen) containing 10% fetal bovine serum. 293T cells were grown in Dulbecco's modified Eagle's medium (Invitrogen) supplemented with 10% fetal bovine serum. The day before transfection, 293 cells were plated in 24-well plates, and were transfected the next day with 20 ng of firefly luciferase reporter plasmid, 5 ng of sea pansy luciferase reporter plasmid (pRL-CMV (Promega)), and expression plasmids (indicated in each figure), by the use of Fugene HD (Roche) according to the

manufacturer's instructions. Total amounts of expression plasmids were adjusted by adding carrier vector. The dual luciferase assays, using the dual-luciferase reporter assay system (Promega), were performed 24 h after transfection according to the manufacturer's instructions. Firefly and sea pansy luciferase activities were quantified by means of a luminometer, with the firefly luciferase activity normalized for transfection efficiency based on the sea pansy luciferase activity. All experiments were done three times.

Colony survival assay. Exponentially growing zebrafish cultured cells were plated at 2 x 10^4 cells per 10-cm dish. The cells were then cultured in L-15 medium not containing phenol red for 15 h. Cells were illuminated with visible light for 3.5 hrs or kept in the dark at room temperature, and then they were irradiated with UV light. Immediately after UV irradiation, cells were illuminated with visible light for 1.5 hrs or kept in the dark at room temperature. Cells were cultured for 12–14 days. Colonies were fixed and stained with 0.3% crystal violet in methanol, and the number of colonies was counted.

Quantitative real-time RT-PCR. Total RNA extraction was done using TRIzol (Invitrogen) according to the manufacturer's instructions. Total RNA was then reverse-transcribed into cDNA by using Superscript II Reverse Transcriptase (Invitrogen) with oligo random hexamers. Each quantitative real-time RT-PCR was performed using the Chromo4 real time detection system (BIO-RAD). PCR primers for *z64Phr* and *zDvl* genes were as follows: z64Phr FW 5'-GAT GAG CAC ATG GAG AGA ACG AAC-3', z64 RW 5'-GTG TCT TCC CTC TGT ACA CGT CTG-3', zDvl FW 5'-CAG ACT ACA TGA GCT CAG CAC GAG-3' and zDvl RW 5'-GTG GAG GAG GTG GAG GCA TCA TAG-3'. The other PCR primers used in this study were described previously.[20,27] For a 20 µl PCR, cDNA template was mixed with the primers to final concentrations of 200 nM and 10 µl of iQ SYBR Green Supermix (BIO-RAD), respectively. The reaction was first incubated at 95°C for 3 min, followed by 40 cycles at 95°C for 15 s, 60°C for 15 s and 72°C for 20 s.

Antibodies. Myc (9E10), p38 and ACTIN antibodies were purchased from Santa Cruz, phospho-p38 and ERK antibodies from Cell Signaling, phospho-ERK, phospho-MEK and MEK antibodies from New England Biolabs, and Flag antibody from Sigma.

Co-immunoprecipitation. Co-immunoprecipitation was done as previously described,[37] with some modifications. 293T cells were seeded in 10-cm dishes, and were transfected the following day with the expression plasmids described in Figure 3. The cells were washed twice with phosphate-buffered saline (PBS) 24 h after transfection, homogenized in binding buffer (150 mM NaCl, 1 mM EDTA, 0.5% Nonidet P-40, 1 mM EGTA, 5% glycerol and 20 mM Tris-HCl pH 7.4) containing protease inhibitor mixture tablets, and then clarified by centrifugation for 10 min at 15,000 x*g*. Total protein from the supernatant was incubated with 15 µl of protein G-agarose beads (Amersham Biosciences) for 1 h at 4°C, after which the material was centrifuged. The supernatant was incubated for 12 h at 4°C with Flag antibody and 20 µl of protein G-agarose bead. The bead was then washed three times with binding buffer, boiled in SDS sample buffer. The supernatant was separated by SDS-PAGE and analyzed by western blotting, as described below.

Western blotting. The immuneprecipitated materials and total cell extracted as described above, was separated by SDS-PAGE and transferred electrophoretically onto a polyvinylidene difluoride membrane. The membrane was blocked with 2% or 5% nonfat milk and incubated with each of antibodies described in each figure for 10 h at 4°C. The blots were incubated with the appropriate secondary antibody, peroxidase-conjugated anti-mouse or anti-rabbit IgG antibody (Santa Cruz), and developed with the ECL western blotting detection system (Amersham Biosciences).

Retroviral infection. The RetroMax expression system (IMGENEX, San Diego, CA) was used to produce retrovirus according to the manufacturer's instructions. Flag-Myc-tagged *z64Phr* gene was cloned into pCLNCX retroviral vector, in which the cloned gene is under the control of CMV promoter. We used pMD.G/vsv-g as enveloping vector. We confirmed the high infection efficiency (95–100%) by pCLNCX retroviral vector expressing GFP and neomycin selection in zebrafish cultured cell.

Acknowledgements

This work was supported by grants of the Yamada Bee Farm, the ministry of Education, Culture, Sports, Science and Technology of Japan (Special Coordination Fund for Promoting Science and Technology and Grant-in-Aid for Young Scientists (Start-up)) to J.H., and by the National Institute of Health to P. S.-C.

Note

Supplementary materials can be found at:
www.landesbioscience.com/supplement/HirayamaCC8-17-Sup.pdf

References

1. Brash DE. UV mutagenic photoproducts in *Escherichia coli* and human cells: a molecular genetics perspective on human skin cancer. Photochem Photobiol 1988; 48:59-66.
2. Mitchell DL, Nairn RS. The biology of the (6-4) photoproduct. Photochem Photobiol 1989; 49:805-19.
3. Sancar A. Cryptochrome: the second photoactive pigment in the eye and its role in circadian photoreception. Annu Rev Biochem 2000; 69:31-67.
4. Sancar A. Structure and function of DNA photolyase and cryptochrome blue-light photoreceptors. Chem Rev 2003; 103:2203-37.
5. Todo T. Functional diversity of the DNA photolyase/blue light receptor family. Mutat Res 1999; 434:89-97.
6. Cashmore AR, Jarillo JA, Wu YJ, Liu D. Cryptochromes: blue light receptors for plants and animals. Science 1999; 284:760-5.
7. Todo T, Ryo H, Yamamoto K, Toh H, Inui T, Ayaki H, et al. Similarity among the Drosophila (6-4)photolyase, a human photolyase homolog, and the DNA photolyase-blue-light photoreceptor family. Science 1996; 272:109-12.
8. Kobayashi Y, Ishikawa T, Hirayama J, Daiyasu H, Kanai S, Toh H, et al. Molecular analysis of zebrafish photolyase/cryptochrome family: two types of cryptochromes present in zebrafish. Genes Cells 2000; 5:725-38.
9. Chaves I, Yagita K, Barnhoorn S, Okamura H, van der Horst GT, Tamanini F. Functional evolution of the photolyase/cryptochrome protein family: importance of the C terminus of mammalian CRY1 for circadian core oscillator performance. Mol Cell Biol 2006; 26:1743-53.
10. Dunlap JC. Molecular bases for circadian clocks. Cell 1999; 96:271-90.
11. Oklejewicz M, Destici E, Tamanini F, Hut RA, Janssens R, van der Horst GT. Phase resetting of the mammalian circadian clock by DNA damage. Curr Biol 2008; 18:286-91.
12. King DP, Takahashi JS. Molecular genetics of circadian rhythms in mammals. Annu Rev Neurosci 2000; 23:713-42.
13. Reppert SM, Weaver DR. Coordination of circadian timing in mammals. Nature 2002; 418:935-41.
14. Okamura H. Clock genes in cell clocks: roles, actions and mysteries. J Biol Rhythms 2004; 19:388-99.
15. Whitmore D, Foulkes NS, Strahle U, Sassone-Corsi P. Zebrafish Clock rhythmic expression reveals independent peripheral circadian oscillators. Nat Neurosci 1998; 1:701-7.

16. Hirayama J, Kaneko M, Cardone L, Cahill G, Sassone-Corsi P. Analysis of circadian rhythms in zebrafish. Methods Enzymol 2005; 393:186-204.
17. Whitmore D, Foulkes NS, Sassone-Corsi P. Light acts directly on organs and cells in culture to set the vertebrate circadian clock. Nature 2000; 404:87-91.
18. Pando MP, Pinchak AB, Cermakian N, Sassone-Corsi P. A cell-based system that recapitulates the dynamic light-dependent regulation of the vertebrate clock. Proc Natl Acad Sci USA 2001; 98:10178-83.
19. Tamai TK, Young LC, Whitmore D. Light signaling to the zebrafish circadian clock by Cryptochrome 1a. Proc Natl Acad Sci USA 2007; 104:14712-7.
20. Hirayama J, Cho S, Sassone-Corsi P. Circadian control by the reduction/oxidation pathway: catalase represses light-dependent clock gene expression in the zebrafish. Proc Natl Acad Sci USA 2007; 104:15747-52.
21. Kelner A. Photoreactivation of ultraviolet-irradiated *Escherichia coli*, with special reference to the dose-reduction principle and to ultraviolet-induced mutation. J Bacteriol 1949; 58:511-22.
22. Kelner A. Effect of visible light on the recovery of Streptomyces griseus conidia from ultraviolet irradiation injury. Proc Natl Acad Sci USA 1949; 35:73-9.
23. Tamai TK, Vardhanabhuti V, Foulkes NS, Whitmore D. Early embryonic light detection improves survival. Curr Biol 2004; 14:104-5.
24. Sancar GB. Enzymatic photoreactivation: 50 years and counting. Mutat Res 2000; 451:25-37.
25. Todo T, Takemori H, Ryo H, Ihara M, Matsunaga T, Nikaido O, et al. A new photoreactivating enzyme that specifically repairs ultraviolet light-induced (6-4)photoproducts. Nature 1993; 361:371-4.
26. Sancar A. Structure and function of photolyase, and in vivo enzymology—50th anniversary. J Biol Chem 2008.
27. Hirayama J, Cardone L, Doi M, Sassone-Corsi P. Common pathways in circadian and cell cycle clocks: light-dependent activation of Fos/AP-1 in zebrafish controls CRY-1a and WEE-1. Proc Natl Acad Sci USA 2005; 102:10194-9.
28. Hara Y, Onishi Y, Oishi K, Miyazaki K, Fukamizu A, Ishida N. Molecular characterization of Mybbp1a as a co-repressor on the Period2 promoter. Nucleic Acids Res 2009.
29. Hirayama J, Fukuda I, Ishikawa T, Kobayashi Y, Todo T. New role of zCRY and zPER2 as regulators of sub-cellular distributions of zCLOCK and zBMAL proteins. Nucleic Acids Res 2003; 31:935-43.
30. Cermakian N, Pando MP, Thompson CL, Pinchak AB, Selby CP, Gutierrez L, et al. Light induction of a vertebrate clock gene involves signaling through blue-light receptors and MAP kinases. Curr Biol 2002; 12:844-8.
31. Pando MP, Sassone-Corsi P. Unraveling the mechanisms of the vertebrate circadian clock: zebrafish may light the way. Bioessays 2002; 24:419-26.
32. Wang Z, Yang H, Tachado SD, Capo-Aponte JE, Bildin VN, Koziel H, et al. Phosphatase-mediated crosstalk control of ERK and p38 MAPK signaling in corneal epithelial cells. Invest Ophthalmol Vis Sci 2006; 47:5267-75.
33. Junttila MR, Li SP, Westermarck J. Phosphatase-mediated crosstalk between MAPK signaling pathways in the regulation of cell survival. Faseb J 2008; 22:954-65.
34. Hirayama J, Nakamura H, Ishikawa T, Kobayashi Y, Todo T. Functional and structural analyses of cryptochrome. Vertebrate CRY regions responsible for interaction with the CLOCK:BMAL1 heterodimer and its nuclear localization. J Biol Chem 2003; 278:35620-8.
35. Cardone L, Hirayama J, Giordano F, Tamaru T, Palvimo JJ, Sassone-Corsi P. Circadian clock control by SUMOylation of BMAL1. Science 2005; 309:1390-4.
36. Ishikawa T, Hirayama J, Kobayashi Y, Todo T. Zebrafish CRY represses transcription mediated by CLOCK-BMAL heterodimer without inhibiting its binding to DNA. Genes Cells 2002; 7:1073-86.
37. Hirayama J, Sahar S, Grimaldi B, Tamaru T, Takamatsu K, Nakahata Y, et al. CLOCK-mediated acetylation of BMAL1 controls circadian function. Nature 2007; 450:1086-90.

J. Biochem. 2009;145(3)345–354
doi:10.1093/jb/mvn172

Blockage by SP600125 of Fcε Receptor-Induced Degranulation and Cytokine Gene Expression in Mast Cells is Mediated Through Inhibition of Phosphatidylinositol 3-Kinase Signalling Pathway

Shuhei Tanemura[1,2], Haruka Momose[1,2,3], Nao Shimizu[1,2], Daiju Kitagawa[1,2], Jungwon Seo[1,2], Tokiwa Yamasaki[1,2], Kentaro Nakagawa[1,2], Hiroaki Kajiho[2], Josef M. Penninger[4], Toshiaki Katada[2] and Hiroshi Nishina[1,*]

[1]Department of Developmental and Regenerative Biology, Medical Research Institute, Tokyo Medical and Dental University, 1-5-45 Yushima, Bunkyo-ku, Tokyo 113-8510; [2]Department of Physiological Chemistry, Graduate School of Pharmaceutical Sciences, The University of Tokyo, 7-3-1 Hongo, Bunkyo-ku, Tokyo 113-0033; [3]Department of Safety Research on Blood and Biological Products, National Institute of Infectious Diseases, Tokyo 208-0011, Japan; and [4]IMBA: Institute of Molecular Biotechnology of the Austrian Academy of Sciences, Dr. Bohrgasse 3, Vienna A-1030, Austria

Received November 25, 2008; accepted December 5, 2008; published online December 23, 2008

SP600125 is used as a specific inhibitor of c-Jun *N*-terminal kinase (JNK). We initially aimed to examine physiological roles of JNK in mast cells that play a central role in inflammatory and immediate allergic responses. We found that Fc receptor for IgE (FcεRI)-induced degranulation (serotonin release) and cytokine gene expression [interleukin (IL)-6, tumour necrosis factor-α and IL-13] in bone marrow-derived mast cells, were almost completely inhibited by SP600125. However, the time course of FcεRI-induced JNK activation did not correlate with that of serotonin release. Furthermore, FcεRI-induced degranulation and cytokine gene expression were not impaired in a JNK activator, MKK7-deficient mast cells, in which JNK activation was lost. These results indicate that the inhibitory effects by SP600125 are not due to impaired JNK activation. Instead, we found that SP600125 markedly inhibited the FcεRI-induced activation of phosphatidylinositol 3-kinase (PI3K) and Akt, the same as a PI3K inhibitor, wortmannin. Finally, we found that SP600125 specifically inhibits delta form of p110 catalytic subunit (p110δ) of PI3K. Thus, SP600125 exerts its influence on mast cell functions by inhibiting the kinase activity of PI3K, but not JNK.

Key words: IgE, JNK, mast cell, PI3K, SP600125.

Abbreviations: Ab, antibody; BMMC, bone-marrow derived mast cell; ERK, extracellular signal-regulated kinase; Gab2, Grb2-associated binder 2; HA, hemagglutinin; IL, interleukin; JNK, c-Jun N-terminal kinase; LPA, lysophophatidic acid; mAb, monoclonal Ab; MKK, MAPK kinase; pAb, polyclonal Ab; PIP3, phosphatidylinositol-3,4,5-triphosphate; SAPK, stress-activated protein kinase; SEK, stress-activated protein kinase/extracellular signal-regulated kinase kinase; TNFα, tumor necrosis factor α.

INTRODUCTION

Mast cells are known to be the main effector cells in the elicitation of the IgE-mediated allergic response. The initiation of an allergic response requires the activation of mast cells and is primarily a consequence of allergen-induced aggregation of the IgE-occupied high-affinity Fc receptor for IgE (FcεRI). Activated mast cells secrete granules, which contain chemical mediators such as proteases, histamine and serotonin, and generate cytokines such as interleukin (IL)-6, IL-13 and tumour necrosis factor (TNF)-α (*1*, *2*). Aggregation of the FcεRI triggers the activation of different signal transduction pathways (*3–6*). Activation of protein tyrosine kinases (PTKs), including Syk, Fyn and Lyn is one of the earliest signalling events induced by aggregation of the FcεRI on mast cells. PTK activation is thought to be proximal to the activation of phosphatidylinositol 3-kinase (PI3K), PKC and calcium signal and appears to be essential for mast cell degranulation (*7*), since PTK inhibitors prevent the liberation of inositol triphosphate and histamine release (*8*, *9*). Both PKC activation and increased intracellular calcium are required for and sufficient for maximal degranulation response.

Another important intermediate is PI3K, which catalyses phosphatidylinositol-3,4,5-triphosphate [PtdIns (3,4,5) P_3] synthesis. PI3K inhibitors abrogate the mast cell calcium response required for degranulation (*10–12*) and impair the activation of mitogen-activated protein kinases (MAPKs) needed for cytokine gene induction (*13*, *14*). Src family tyrosine kinase, Fyn and scaffolding adaptor protein Grb2-associated binder 2 (Gab2) are important molecules to relay the signal from FcεRI to PI3K in mast cells. Fyn binds and phosphorylates Gab2 on FcεRI aggregation and phosphorylated Gab2 binds and activates PI3Ks. Since mast cells lacking Fyn or Gab2 are severely impaired in degranulation and cytokine production, the Fyn-Gab2-PI3K pathway is

*To whom correspondence should be addressed. Tel: +81-3-5803-4659; Fax: +81-3-5803-5829; E-mail: nishina.dbio@mri.tmd.ac.jp

a necessary signal for mast cell function. PI3Ks activated by the FcεRI include the heterodimeric class IA PI3Ks, which consist of a p110α, p110β or p110δ catalytic subunit bound to either one of five regulatory proteins (p85α, p55α, p50α, p85β or p55γ) that link the p110 subunits to tyrosine kinase signalling pathways. However, the specific role for each of the three class IA PI3K catalytic subunits has not been determined.

Aggregation of the FcεRI also activates MAPKs including extracellular signal-regulated kinase (ERK), p38 MAPK and c-Jun N-terminal kinase (JNK)/stress-activated protein kinase (SAPK). JNK is activated not only by many types of cellular stresses including UV irradiation, heat shock, but also by certain cytokines and mitogens. In hematopoietic cells, JNK is thought to play an important role for cytokine production through their regulation of transcription. The activated JNK phosphorylates a number of substrates including c-Jun, a component of the activator protein-1 (AP-1) transcription factor, to regulate gene expression for the stress responses and immune responses. JNK also regulates various cellular functions independent of transcription regulation (*15–17*). In MAP kinase family, ERK and p38 were reported to be important in cytokine expression and degranulation by the inhibitor study in FcεRI-activated mast cells (*18–21*). MAPK kinase (MKK) 7 directly phosphorylates and activates JNK. We previously showed MKK7-deficient mast cells hyperproliferate in response to growth factor stimulation, suggesting that JNK signalling plays an important role in mast cell homeostasis (*22*). In contrast, physiological role of FcεRI-induced JNK activation in mast cells is still unclear. Recently, many researchers use a specific inhibitor, SP600125 (*15*, *23*, *24*). Under this situation, we thought to use both pharmacological approach using SP600125 and genetical approach using *mkk7*-deficient mast cells to reveal the role of JNK activation in FcεRI-activated mast cells.

In this report, we found that SP600125 abrogates Fcε-induced degranulation and cytokine gene expression. Unexpectedly, SP600125 exerts its influence on mast cell function by inhibiting the kinase activity of PI3K but not JNK.

MATERIALS AND METHODS

Materials—The anti-JNK1 (C-17), anti-JNK1 (FL), anti-JNK2 (FL), anti-Fyn (FYN3), anti-Fyn (15), anti-Lyn (44), anti-Lyn (H-6), anti-Akt1/2 (N-19), anti-Akt1 (C-20) and anti-p110α (c-17) Abs were purchased from Santa Cruz Biotechnology, Inc. The anti-Phosphotyrosine (4G10) was from Upstate Biotechnology, Inc. Anti-phospho-SAPK/JNK (9251), anti-phospho-ERK (9106) and anti-phospho-Akt (9271) Abs were purchased from Cell Signaling Technology, Inc. Anti-Shc antibody was from BD Transduction Laboratories. Anti-FLAG (M2) agarose, anti-DNP IgE Ab (SPE-7), DNP–HSA, adenosine, A23187, anisomycin and Thapsigargin were purchased from Sigma-Aldrich Co. PD98059, LY294002 and PP2 were purchased from Calbiochem. SP600125 and wortmannin were from BIOMOL International, L.P. and Wako Pure Chemical Industries, Ltd, respectively. Horseradish peroxidase-labelled anti-rabbit IgG was from Jackson ImmunoResearch Laboratories, Inc. All other reagents were analytical grade and were obtained from commercial sources.

Mast Cell Preparation—Bone marrow cells were flushed from femurs of mice. Cells were washed twice with PBS and resuspended at 5×10^5/ml in culture medium (OptiMEM medium supplemented with 10% FCS, 50 μM β-mercaptoethanol, antibiotics (GIBCO/BRL) and 2 ng/ml IL-3 (Genzyme). FcεRI$^+$ c-Kit$^+$ Bone marrow-derived mast cells (BMMCs) were prepared by continuous transfer of cells growing in suspension as described (*22*). On the other hand, MKK7-deficient FcεRI$^+$ c-Kit$^+$ mast cells were prepared from fetal liver cells of *mkk7*$^{-/-}$ mice (*25*). *mkk7*$^{-/-}$ fetal liver cells at embryonic date 11.5 (E11.5) were cultured in the presence of IL-3 the same as BMMCs.

Flow Cytometry—For the measurement of FcεRI and c-Kit, Cells were incubated with 1 μg/ml anti-TNP IgE (BD PharMingen) for 50 min, washed with culture medium and then incubated with FITC-conjugated anti-mouse IgE (BD PharMingen) and PE-conjugated anti-c-Kit mAb (BD PharMingen) for 30 min. Flow cytometric analysis of the stained cells was performed with FACScan or FACSCalibur (Becton–Dickinson) equipped with CellQuest software.

Degranulation Assay—The degree of degranulation was determined by measuring the release of serotonin. Cells (1×10^6 cells/ml) were sensitized for 3 h at CO_2 incubator with anti-DNP IgE (1 μg/ml) and [^{3}H] serotonin in culture medium without IL-3. Sensitized cells were washed twice with starvation medium (OptiMEM medium supplemented with 50 μM β-mercaptoethanol and 0.1% BSA) and then resuspended at 5×10^6 cells/200 μl. Cells were preincubated for 15 min with inhibitor and then stimulated with DNP–HSA for 15 min. Samples were put on ice and centrifuged 8.8×10^3 r.p.m. for 2 min. Release of [^{3}H] serotonin to supernatant was measured in triplicate by liquid scintillation and results are described as the percent of degranulation.

Northern Blot Analysis—Cells (6×10^6 cells/ml) were sensitized for over night at CO_2 incubator with anti-DNP IgE (1 μg/ml) in starvation medium. Sensitized cells were washed twice with starvation medium and then resuspended at 1.2×10^7 cells/4.8 ml. Cells were preincubated for 15 min with inhibitor and then stimulated with DNP–HSA for indicated time. Total RNA from BMMCs was prepared using Trizol reagent (Sigma-Aldrich), separated by formamide agarose gel, and transferred to a Hybond-XL (Amersham Biosciences). IL-6, IL-13, TNF-α and β-actin were detected by Northern blotting using the specific DNA probes. The cDNA fragments corresponding to mouse IL-6, IL-13, TNF-α and β-actin were amplified using the following primers: IL-6, 5′-ATG AAG TTC CTC TCT GCA AGA GAC T-3′ and 5′-CAC TAG GTT TGC CGA GTA GAT CTC-3′, IL-13, 5′-AAT GAA TTC ATG GCG CTC TGG GTG -3′ and 5′-ATA GTC GAC TTA GAA GGG GCC G-3′, TNF-α, 5′-GGC AGG TCT ACT TTG GAG TCA TTG C-3′ and 5′-ACA TTC GAG GCT CCA GTG AAT TCG G-3′, β-actin, 5′-CAT CAC TAT TGG CAA CGA GC-3′ and 5′-ACG CAG CTC AGT AAC AGT CC-3′.

Immunoblotting and Immunoprecipitation—Cells (1×10^6 to 6×10^6 in 1 ml) were sensitized for 3 h with anti-DNP IgE (1 μg/ml) in culture medium (without IL-3). Sensitized cells (2.5×10^6 to 10×10^6 in 1 ml) were preincubated with inhibitor and stimulated with DNP–HSA (10 ng/ml) for indicated time. Cells were pelleted by centrifugation and resuspended in ice cold lysis buffer (1% NP-40, 20 mM HEPES, pH 7.4, 150 mM NaCl, 5 mM EDTA, 50 mM NaF, 0.05% 2-mercaptoethanol, 1 mM phenylmethylsulfonyl fluoride, and 100 μM Na_3VO_4, 4 μg/ml aprotinin). The detergents used for Shc immunoprecipitation were 1% NP-40, 0.5% deoxicholate, and 0.1% SDS. Abs used for immunoprecipitation were anti-Shc, anti-Fyn (FYN3), anti-Lyn (44), anti-p110α (c-17), anti-Akt1 (c-20) and anti-JNK (c-17). Immunoprecipitations and immunoblotting were carried out by using standard procedures (*26*).

JNK Kinase Assay—For detection of JNK kinase activity, total JNKs were immunoprecipitated (2 h, 4°C) from BMMC lysates using polyclonal rabbit anti-JNK IgG reactive against all JNK isoforms. Immune complexes were harvested on protein A-Sepharose beads. And the *in vitro* kinase assay was performed with enolase as a substrate by the method described previously (*26*).

Akt Kinase Assay—For detection of Akt kinase activity, total Akts were immunoprecipitated (2 h, 4°C) from BMMC lysates using polyclonal rabbit anti-Akt Ab (C-20; Santa Cruz Biotechnology, Inc.). Immune complexes were harvested on protein G-Sepharose beads. For kinase assays, immune complexes were washed three times with TBS 0.1% NP-40. The beads were resuspended in 20 μl kinase buffer (10 mM $MgCl_2$, 50 mM HEPES, 0.01% NP-40, 1 mM DTT) and Akt activity was assayed at 30°C for 20 min in the presence of 4 μCi [γ-^{32}P] ATP using 1 μg of GST-GSK3β as the *in vitro* substrate. The reaction was stopped by the addition of 4× SDS sample buffer. GST-GSK3β phosphorylation was visualized by autoradiography as described previously (*26*).

Src Family Kinase Assay—293T cells were transfected with pME/Flag-Fyn or pME/Lyn using LipofectAMINE 2000 (Invitrogen). Cell lysates were immunoprecipitated (2 h, 4°C) using polyclonal rabbit anti-Lyn or Fyn (Santa Cruz Biotechnology, Inc.). Immune complexes were harvested on protein A-Sepharose beads. And the *in vitro* kinase assay was performed with enolase as a substrate as described previously (*27*).

PI3K Kinase Assay—The cDNA encoding mouse p110 α or p110 δ were cloned into mammalian expression vector pCMV5-Flag. 293T cells were transfected with pCMV5-Flag p110 α or p110 δ using LipofectAMINE 2000 (Invitrogen). PI3K activity was measured described previously (*22*). Briefly, the immunoprecipitates containing PI3K were washed with TBS and suspended in 25 μl of a kinase buffer consisting of 40 mM Tris–HCl (pH 7.4), 1 mM EGTA (pH 7.5), 0.2 mM phosphatidylinositol 4, 5-bisphosphate and 0.2 mM phosphatidylserine and incubated with or without 1 μM wortmannin at 30°C for 15 min. After addition of 10 μl ATP solution (25 mM $MgCl_2$, 0.5 mM ATP, and 10 μCi of [γ-^{32}P]ATP), the immunoprecipitates were further incubated for 15 min. The reaction was terminated by adding 470 μl of chloroform/methanol/8% $HClO_4$ (30:60:4) and mixed with 50 μl of water and 150 μl each of chloroform and 8% $HClO_4$. The lipid phase separated by centrifugation was washed twice with chloroform-saturated 0.5 M NaCl containing 1% $HClO_4$ and dried. The extracted lipid was dissolved in 20 μl of chloroform/methanol (95:5) and spotted on a TLC plate (Silica gel 60, Merck). Prior to spotting, the plate was once developed with methanol/water (2:3) containing 1.2% potassium oxalate and pre-activated by heating at 110°C for 20 min. The plate was developed in chloroform/acetone/methanol/acetic acid/water (80:30:26:24:14), and radioactivity was visualized with the bioimaging analyzer as described previously (*28*).

Assays for PIP3 Production—PIP3 production was measured according to the method described by Momose *et al.* (*28*). Cells (1×10^6 cells/ml) were over night sensitized at CO_2 incubator with anti-DNP IgE (1 mg/ml) in culture medium without IL-3.The sensitized BMMCs were suspended at the density of 4×10^7 cells/ml in a labeling medium consisting of 10 mM HEPES–NaOH (pH 7.4), 136 mM NaCl, 4.9 mM KCl and 5.5 mM glucose, and incubated at 37°C for 30 min with 500 mCi/ml of ^{32}Pi. The radiolabelled cells were washed twice with the same medium and resuspended at 5×10^6 cells/ml in the medium containing 1 mM $CaCl_2$. Aliquots (400 ml, 2×10^6 cells/ml) were preincubated for 5 min and further incubated with the indicated reagents. The reaction was terminated by the addition of 1.55 ml of chloroform/methanol/8% $HClO_4$ (50:100:5). Then 0.5 ml each of chloroform and 8% $HClO_4$ were added to the mixture, and the lipid phase was separated by centrifugation. The lipid phase was washed with chloroform-saturated 1 M NaCl containing 1% $HClO_4$ and dried. The procedure after this step was performed by the method described in *PI3K kinase assay* (*28*).

RESULTS

SP600125 Inhibits FcεRI-Induced Degranulation in BMMC—We first examined the effect of SP600125 on FcεRI-induced degranulation. After BMMCs were sensitized by the incubation with IgE for 3 h, they were pretreated with inhibitors for 15 min and stimulated with DNP–HSA for 15 min, and finally measured a serotonin release as the extent of degranulation. As expected, a PI3K inhibitor, wortmannin completely inhibited FcεRI-induced serotonin release in a dose-dependent manner (Fig. 1A). An ERK kinase (MEK) inhibitor, PD98059 and a p38 kinase inhibitor, SB203580 partially inhibited the serotonin release (Fig. 1B and C). In contrast, a JNK inhibitor, SP600125 almost completely inhibited FcεRI-induced serotonin release (Fig. 1D). These results clearly show that SP600125 inhibits FcεRI-induced degranulation in BMMC the same as PI3K inhibitor, wortmannin.

SP600125 Inhibits FcεRI-Induced Cytokine Gene Expression in BMMC—We next examined the effect of SP600125 on FcεRI-induced cytokine gene expression. Sensitized BMMCs were pretreated with inhibitors for 15 min and stimulated with DNP–HSA for 60 min. Total RNAs were extracted from cells and were analysed by Northern blotting. Wortmannin completely inhibited

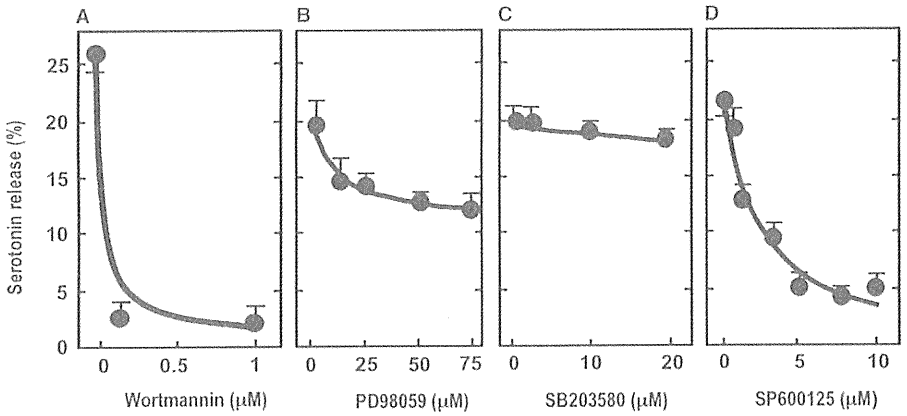

Fig. 1. **Inhibition of FcεRI-induced serotonin release by SP600125 in BMMCs.** BMMCs were sensitized with IgE for 3 h and were preincubated in the presence of indicated concentrations of (A) Wortmannin, (B) PD98059, (C) SB203580, (D) SP600125 and stimulated with 10 ng/ml of DNP–HSA for 15 min. Serotonin release was measured as described in MATERIALS AND METHODS.

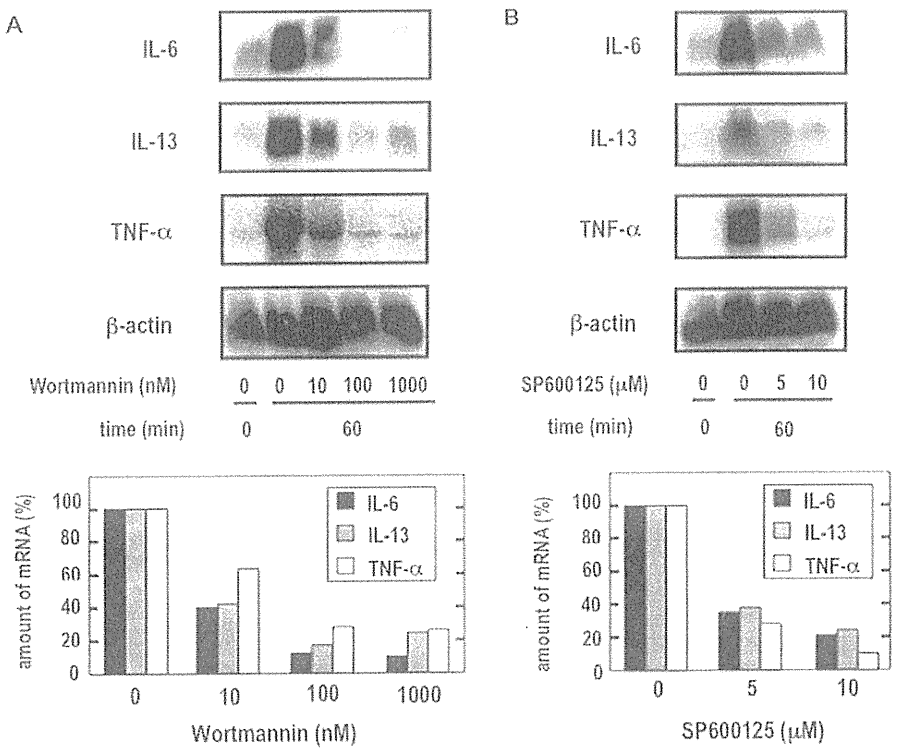

Fig. 2. **Inhibition of FcεRI-induced cytokine gene expression by SP600125 in BMMCs.** BMMCs were sensitized over night with IgE. Sensitized BMMCs were preincubated for 15 min in the presence of (A) wortmannin or (B) SP600125 and stimulated with DNP–HSA for 60 min. mRNA was purified from cells and cytokine mRNAs were detected by northern blotting. Upper panel, autoradiography; lower panel, quantitation of specific cytokines.

gene expression of IL-6, IL-13 and TNF-α in a dose-dependent manner (Fig. 2A). SP600125 also inhibited cytokine gene expression the same as wortmannin (Fig. 2B). These results clearly show that SP600125 inhibits FcεRI-induced cytokine gene expression in BMMC the same as PI3K inhibitor, wortmannin.

FcεRI-Induced Degranulation Occurs Before JNK Activation in BMMC—As SP600125 inhibited FcεRI-induced mast cell function severely, we further investigated a relationship between FcεRI-induced degranulation and JNK activation. Sensitized BMMCs were stimulated with DNP–HSA for indicated time and JNK

activity was measured (Fig. 3A). Unexpectedly, FcεRI-induced JNK activation started at 8 min after stimulation. A time-course of FcεRI-induced degranulation was much faster than that of JNK activation (Fig. 3B).

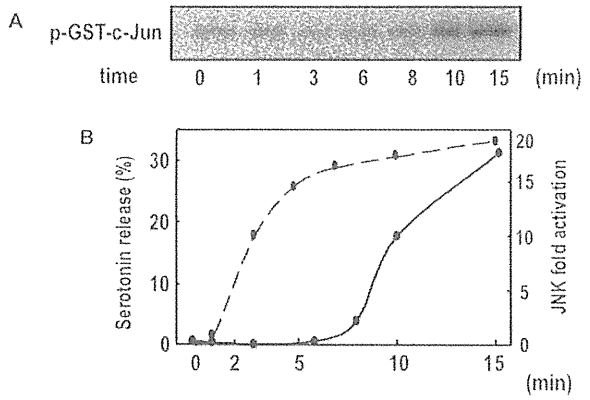

Fig. 3. **A time course of FcεRI-induced JNK activation and serotonin release.** (A) Time course of FcεRI-induced JNK activation. BMMCs were sensitized with anti-DNP IgE and stimulated with DNP–HSA for indicated time periods. Lysates from these cells were immunoprecipitated with an anti- JNK (C-17) Ab. Immunoprecipitated JNK activity in the precipitated fractions were measured using GST-c-Jun as a substrate in the presence of [γ-^{32}P] ATP as described in MATERIALS AND METHODS. (B) Comparison of FcεRI-induced JNK activation and serotonin release. Solid line shows a time course of quantified JNK activation in (A) and dotted line shows time course of FcεRI-induced serotonin release.

These results indicates that FcεRI-induced degranulation is independent of JNK activation.

SP600125 Inhibits FcεRI-Induced Degranulation in MKK7-Deficient Mast Cells—To address the relationship between FcεRI-induced mast cell function and JNK activation, we prepared MKK7-deficient mast cells, which expressed both FcεRI and c-Kit (FcεRI$^+$ c-Kit$^+$). Fetal liver derived mast cells (FLMCs) were prepared from *mkk7*$^{-/-}$ embryos at E11.5. Both wild-type (*mkk7*$^{+/+}$) and *mkk7*$^{-/-}$ FLMCs expressed FcεRI and c-Kit (Fig. 4A). Sensitized FLMCs were stimulated with DNP–HSA and cell lysates were subjected to Western blot analysis. FcεRI-induced ERK activation was equivalent in both wild-type and *mkk7*$^{-/-}$ FLMCs (Fig. 4B). In contrast, FcεRI-induced JNK activation was completely lost in *mkk7*$^{-/-}$ FLMCs (Fig. 4B). So, we used these cells to examine relationship between FcεRI-induced mast cell function and JNK activation. Wild-type and *mkk7*$^{-/-}$ FLMCs were stimulated with DNP–HSA for 15 min and serotonin release was measured. FcεRI-induced serotonin release was comparable in wild-type and *mkk7*$^{-/-}$ FLMCs (Fig. 4C). Wild-type and *mkk7*$^{-/-}$ FLMCs were sensitized with IgE and stimulated with DNP–HSA for indicated time, and then RNAs from these cells were subjected to Northern blot analysis. Gene expression of IL-6, IL-13 and TNFα was almost the same in wild-type and *mkk7*$^{-/-}$ FLMCs (Fig. 4E). Interestingly, SP600125 inhibits FcεRI-induced serotonin release in MKK7-deficient mast cells (Fig. 4D). These results clearly show that the inhibitory effect of SP600125 on FcεRI-induced mast cell function is independent of

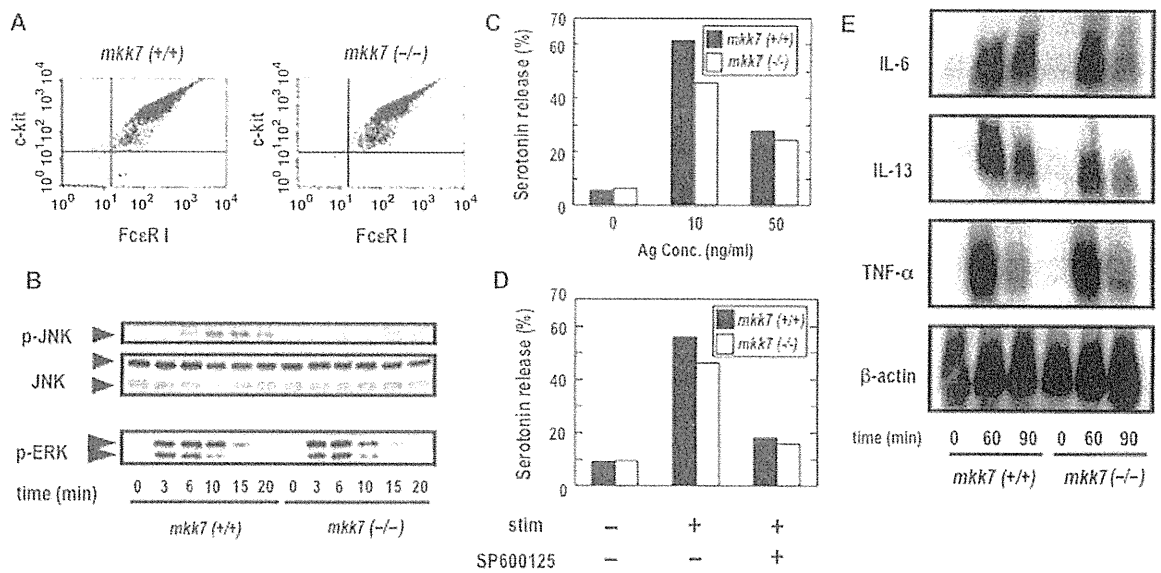

Fig. 4. **FcεRI-induced mast cell function in wild-type and *mkk7*$^{-/-}$ mast cells.** A: Cell surface expression of the high-affinity IgE receptor (FcεRI) and c-Kit in FLMCs were analysed by FACS. *mkk7*$^{+/+}$ and *mkk7*$^{-/-}$ FLMCs were incubated with anti-TNP IgE mAb and then incubated with FITC-anti-mouse IgE and PE-anti-Kit Abs followed by flow cytometry. B: *mkk7*$^{+/+}$ and *mkk7*$^{-/-}$ FLMCs were sensitized with anti-DNP IgE (1 μg/ml) for 3 h and then stimulated with DNP–HSA (10 ng/ml) for the indicated time period. Total lysates from these cells were resolved on SDS–PAGE, transferred to PVDF membrane filters, and then immunoblotted with anti-phospho-SAPK/JNK Ab, anti-JNK Ab and anti-phospho-ERK Ab. C and D: FLMCs were sensitized for 3 h with anti-DNP IgE and then stimulated with DNP–HAS. Serotonin release was measured. E: FLMCs were sensitized over night with anti-DNP IgE and then stimulated with DNP–HSA. mRNA was purified from cells and cytokine mRNAs were detected by Northern blotting.

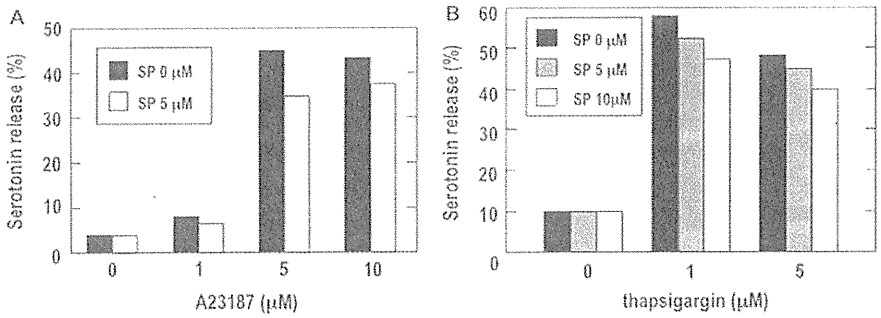

Fig. 5. **Effects of SP600125 on A23187- or thapsigargin-induced serotonin release in BMMCs.** IgE sensitized BMMCs were preincubated in the presence of indicated concentrations of SP600125 for 15 min and stimulated with (A) A23187 or (B) thapsigargin for 15 min. Serotonin release was determined as described in MATERIALS AND METHODS.

JNK activation. Thus, SP600125 has another target molecule(s) other than JNK in mast cells.

The Target Molecule of SP600125 is Located Upstream of Calcium Signalling in FcεRI-Induced Signalling Pathway—To address the target molecule(s), we examined whether the target of SP600125 was located upstream or downstream of Calcium signalling. BMMCs were treated with 5 μM of SP600125 or DMSO for 15 min and stimulated with various concentrations of Calcium ionophore A23187 or Thapsigargin, which elevates cytosolic Calcium concentration by inhibiting the Calcium channel in ER, for 15 min. SP600125 could not inhibit both A23187-induced and thapsigargin-induced serotonin release in BMMCs (Fig. 5). These results indicate that the target molecule(s) of SP600125 is located upstream of Calcium signalling in mast cells.

Syk and Src Family Tyrosine Kinases are Not Target Molecules of SP600125—Like all immunoreceptor family members, FcεRI lacks intrinsic tyrosine kinase activity. Agtigen-induced crosslinking of FcεRI initiates a complex series of phosphate transfer events via the activation of Syk and Src family protein tyrosine kinases and deficiency of these kinases lead to severe defect in mast cell function. To examine the effect of SP600125 on Syk, we checked the phosphorylation of Shc, which is phosphorylated by Syk in response to FcεRI-induce stimulation (Fig. 6A). Sensitized BMMCs were pretreated with various concentrations of SP600125 or DMSO and stimulated with DNP–HSA. Lysate prepared from BMMCs was immnoprecipitated by anti-Shc Ab, and immunoblotted with anti-phospho-Tyr antibody. There were almost no different FcεRI-induced Shc phosphorylation between SP600125- and DMSO-treated BMMCs. These results indicate that Syk is not a target molecule of SP600125 in FcεRI-induced signalling pathway.

To examine the effect of SP600125 on Src family, Fyn and Lyn, we directly measured kinase activities of Fyn and Lyn using enolase as a phosphorylation substrate. Recombinant Fyn and Lyn were immunoprecipitated from 293T cells and subjected to *in vitro* kinase assay (Fig. 6B). A Src faimly kinase inhibitor, PP2 efficiently inhibited phosphorylation of enolase. However, SP600125 could not inhibit phosphorylation of enolase by Lyn and Fyn. Inhibitory specificities of SP600125 and PP2 were confirmed by the *in vitro* JNK kinase assay (Fig. 6C). These results indicate that Src family members, Fyn and Lyn are not direct target molecules of SP600125.

SP600125 Inhibits FcεRI-Induced PI3K Activation in BMMCs—We examined the effect of SP600125 on PI3K activation in two ways. First, sensitized BMMCs were pretreated with SP600125 or DMSO control and stimulated with DNP–HSA for indicated time. Total lysates prepared from BMMCs were subjected to Western blot anlysis using anti-phospho-Akt Ab. As shown in Fig. 7A, Akt was Tyr phosphorelated in control cells, however, the Tyr phoshorylation of Akt was completely diminished in SP600125-treated cells. Secondly, we measured the intracellular accumulation of PIP_3 in FcεRI-activated BMMCs by TLC chromatography. As shown in Fig. 7B, PIP_3 production was detected in control (DMSO) cells, however, was not detected in cells treated with SP600125 or wortmannin. These results clearly show that SP600125 inhibits FcεRI-induced PI3K activation.

SP600125 Specifically Inhibits IgE Receptor but Not Adenosine Receptor-Mediated PIK3 Signalling Pathway in BMMCs—It is well known that mast cells have adenosine receptor on its cell surface and produces PIP3 through PI3Kγ in response to adenosine stimulation. To examine specificities of PI3K isoforms, we examined the effect of SP600125 on FcεRI- or adenosine-induced PI3K activation in BMMCs (Fig. 8). We used Akt kinase assay to evaluate the activation of PI3K quantitatively. BMMCs were pretreated with various concentrations of SP600125 or DMSO and stimulated with DNP–HSA or adenosine. Lysates prepared from BMMCs were immnoprecipitated by anti-Akt Ab and were subjected to Akt kinase assay. Interestingly, adenosine-induced Akt activation was affected partially by SP600125 pretreatment, however, FcεRI-induced Akt activation was greatly impaired. These results indicate that SP600125 inhibits a specific isoform(s) of PI3K family members.

SP600125 Specifically Inhibits Delta Type of PI3K Isoform—Finally, we investigate whether the SP600125 directly inhibits PI3K the same as wortmannin and LY294002. We cloned p110α isoform, which express ubiquitously, and p110δ isoform, which is primarily found in leucocytes, from mast cell cDNA library. Flag tagged p110α or p110δ transfected to 293T cells were immunoprecipitated by anti-Flag Ab and subjected to

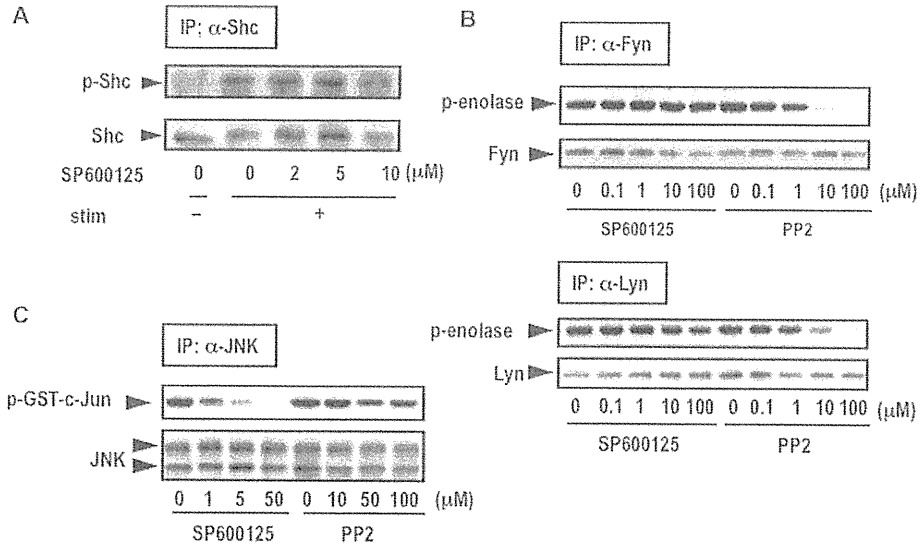

Fig. 6. **Effects of SP600125 on Shc phosphorylation and kinase activities of Src family tyrosine kinases.** A: IgE-sensitized BMMCs were preincubated in the presence of indicated concentrations of SP600125 and stimulated with DNP–HSA for indicated time periods. Lysates from these cells were immunoprecipitated with anti-Shc Ab. Immunoprecipitated, proteins were resolved on SDS–PAGE, transferred to PVDF membrane filters, and then immunoblotted with anti-phosphotyrosine Ab (upper lanes) and anti-Shc Ab (lower lanes). B: 293T cells were transfected with pME/Flag-Fyn or pME/Lyn. The transfected 293T cells, after being cultured for 48 h, were lysed and Fyn and Lyn were immunoprecipitated with anti-Fyn and anti-Lyn Abs. Inhibitory effect of SP600125 was measured by kinase activities of immunoprecipitated Fyn and Lyn with acid-treated enolase as a substrate in the presence of inhibitor and [γ-^{32}P] ATP. The insets show the ^{32}P-phosphorylated enolase (upper lanes) and precipitated kinases (lower lanes). C: Hela cells were stimulated with anisomycin (10 μg/ml) for 30 min. Cell lysates were prepared from the stimulated cells and immnoprecipitated with an anti-SAPK/JNK (C-17) Ab. Inhibitory effect of SP600125 was assessed by measuring immunoprecipitated SAPK/JNK activity with GST-c-Jun as a substrate in the presence of inhibitor and [γ-^{32}P] ATP. The insets of panels show the ^{32}P-phosphorylated GST-c-Jun (upper lanes) and precipitated kinases (lower lanes).

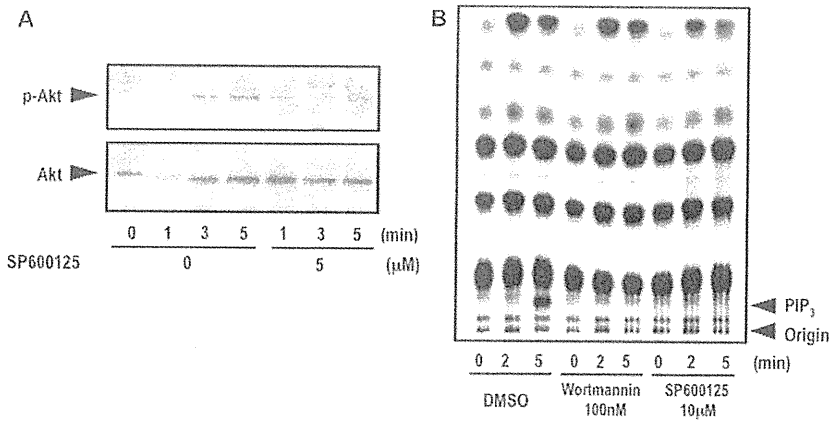

Fig. 7. **Effects of SP600125 on FcεRI-induced PI3K activation and PIP_3 production.** A: IgE sensitized BMMCs were preincubated in the presence of indicated concentrations of SP600125 and stimulated with DNP–HSA for indicated time periods. Lysates from these cells were resolved on SDS–PAGE, transferred to PVDF membrane filters, and then immunoblotted with anti-phospho-Akt Ab (upper lanes) and anti-Akt Abs (lower lanes). B: Sensitized BMMCs were labelled with ^{32}P-orthophosphate. Then, these cells were pretreated with wortmannin or SP600125 for 15 min and stimulated with DNP–HSA for indicated time periods. Lipids were extracted from these cells and separated by thin-layer chromatography.

in vitro kinase assay. As shown in Fig. 9, PIP3 production in Flag-p110α immunoprecipitants were not affected by SP600125. In contrast, SP600125 severely inhibited PIP3 production in the Flag-p110δ immunoprecipitants. This result indicates that SP600125 specifically inhibits p110δ rather than p110α.

DISCUSSION

In this study, we found that FcεRI-induced degranulation and cytokine gene expression including IL-6, TNF-α and IL-13 were almost completely inhibited by a well-known JNK inhibitor, SP600125 in BMMCs (Figs 1 and 2).

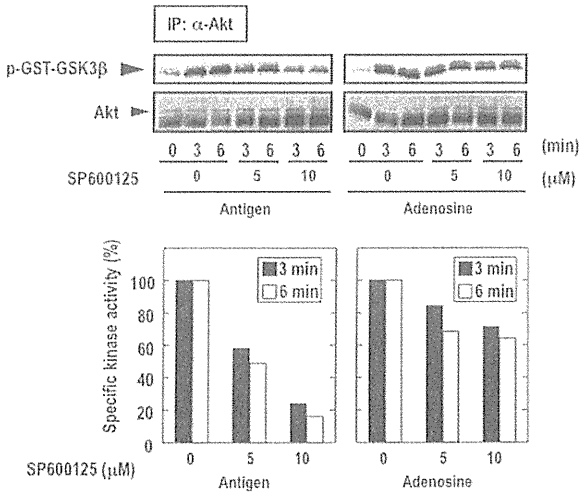

Fig. 8. **Effects of SP600125 on FcεRI- or adenosine-induced Akt activation.** BMMCs were pretreated with various concentrations of SP600125 and then stimulated with FcεRI or adenosine for indicated time periods. Lysates from these cells were immunoprecipitated with anti-Akt Ab. Kinase activities of immunoprecipitated Akt in the precipitated fractions were measured with GST-GSK3β as a substrate in the presence of [γ-^{32}P] ATP. The insets of panels show the ^{32}P-phosphorylated GST-GSK3β (upper lanes) and precipitated Akt (lower lanes). Lower panels show the Akt kinase activity, which expressed as the percentage compared with the control level observed in 0 μM of SP600125 in each time period.

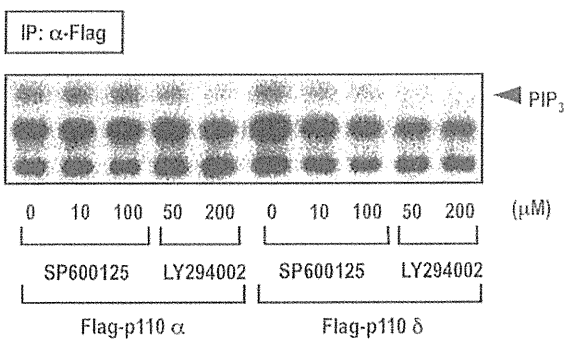

Fig. 9. **Effects of SP600125 on PI3Ks, p110α and p110δ *in vitro*.** 293T cells were transfected with pCMV/Flag-p110α or pCMV/Flag-p110δ. The transfected 293T cells, after being cultured for 48 h, were lysed and immunoprecipitated with anti-FLAG (M2) agarose. Inhibitory effects of SP600125 were assessed by measuring immunoprecipitated p110 α/δ activity with PIP2 as a substrate in the presence of inhibitor and [γ-^{32}P] ATP as described in MATERIALS AND METHODS.

However, the time course of JNK activation did not correlate with that of Fcε-induced degranulation (Fig. 3). FcεRI-induced degranulation and cytokine gene expression were not impaired in MKK7-deficient mast cells, which lost JNK activation (Fig. 4). Furthermore, SP600125 inhibited FcεRI-induced degranulation in MKK7-deficient mast cells (Fig. 4). These results clearly show that the impaired phenotypes observed by SP600125 treatment are not due to impaired JNK activation. Instead, we found that SP600125 markedly inhibited the activation of PI3K and Akt (Fig. 7), but did not inhibit Syk and Src family tyrosine kinases (Fig. 6). Finally, we found that SP600125 specifically inhibit delta isoform of PI3K, which is recently revealed to be an important molecule in FcεRI-signalling in mast cells (Fig. 9).

We have shown that MKK7 is essential for JNK activation and that MKK7 negatively regulate the proliferation of mast cells using MKK7-deficient mast cells (*22*). Therefore, we examined the role of MKK7-JNK signalling in FcεRI-induced mast cell function. Indeed, FcεRI-induced JNK activation in MKK7-deficient mast cells was lost (Fig. 4B). However, there were no differences of mast cell function between wild-type and MKK7-deficient mast cells.

SP600125 was originally reported as a specific and reversible ATP-competitive inhibitor for JNK and has been used to study JNK signal in cellular context. Bain *et al.* (*29*) previously reported that SP600125 inhibits several kinds of kinases *in vitro*. In the present work, we also showed that SP600125 inhibit p110δ isoform of class IA PI3K besides JNK and impaired mast cell function. Unlike the ubiquitously expressed p110α and p110β, the p110δ isoform is primarily expressed in leucocytes. Therefore, it would be better to take care of using SP600125 as a specific JNK inhibitor in leucocytes. Other JNK inhibitors, such as CEP1347 and small peptide inhibitor I-JIP, may be useful for studying JNK function in leucocytes.

Among the different isoforms of PI3K, the class I variant is activated after FcεRI aggregation. Class I PI3Ks are further subdivided into two groups. Class IA PI3Ks consist of p110α, β or δ catalytic subunit and link to the family of receptor tyrosine kinases. Class IB PI3K consists of p110γ catalytic subunit and link to the family of G-protein-coupled receptors. We examined the effect of SP600125 on adenosine-receptor-induced PI3K activation, because adenosine receptor is a G-protein-coupled receptor (GPCR) and activates class IB PI3Kγ. However, we found that SP600125 did not inhibit adenosine-induced activation of PI3K (Fig. 8). We also examined the effect of SP600125 on IL-3 and SCF, and found that SP600125 severely inhibited IL-3 or SCF-induced PI3K activation the same as FcεRI (data not shown). IL-3 and SCF receptors belong to the family of receptor tyrosine kinase but not GPCR family. Thus, SP600125 inhibit Class IA type PI3K, p110δ but not class IB type PI3Kγ. Recent study indicated that p110δ isoform is the main component of the PI3K-dependent antigen-IgE signalling cascade leading to degranulation and cytokine production. Although wortmannin and LY294002 are well used and are powerful inhibitors of PI3K, there is no specificity among the four members of the class I PI3K. Therefore, we show the possibility that SP600125 and its derivatives may be useful as specific inhibitor of p110δ isoform.

SP600125 was reported to suppress bronchoalveolar accumulation of eosinophils and lymphocytes in animals subjected to repeated allergen exposure (*24*). Cytokines, proteases, biogenic amines and lipid mediators secreted

from mast cells were known to induce basophils and eosinophils to inflammatory tissues. So, FcεRI-activated mast cells contribute to leucocyte infiltration. Therefore, the effect of SP600125 in model animal, in part, may be explained by impaired PI3K signalling in mast cells.

ACKNOWLEDGEMENTS

We are grateful to numerous members of the Nishina and Katada Laboratories for critical reading and helpful discussions.

FUNDING

This work was supported in part by research grants (to H.N) from the Ministry of Education, Culture, Sports, Science and Technology (MEXT) of Japan, and the Japanese Society for the Promotion of Science (JSPS).

CONFLICT OF INTEREST

None declared.

REFERENCES

1. Wedemeyer, J., Tsai, M., and Galli, S. J. (2000) Roles of mast cells and basophils in innate and acquired immunity. *Curr. Opin. Immunol.* **12**, 624–631
2. Marone, G., Galli, S. J., and Kitamura, Y. (2002) Probing the roles of mast cells and basophils in natural and acquired immunity, physiology and disease. *Trends Immunol.* **23**, 425–427
3. Kinet, J. P. (1999) The high-affinity IgE receptor (Fc epsilon RI): from physiology to pathology. *Annu. Rev. Immunol.* **17**, 931–972
4. Kawakami, T. and Galli, S. J. (2002) Regulation of mast-cell and basophil function and survival by IgE. *Nat. Rev. Immunol.* **2**, 773–786
5. Siraganian, R. P. (2003) Mast cell signal transduction from the high-affinity IgE receptor. *Curr. Opin. Immunol.* **15**, 639–646
6. Galli, S. J., Kalesnikoff, J., Grimbaldeston, M. A., Piliponsky, A. M., Williams, C. M. M., and Tsai, M. (2005) Mast cells as "tunable" effector and immunoregulatory cells: recent advances. *Annu. Rev. Immunol.* **23**, 749–786
7. Ozawa, K., Szallasi, Z., Kazanietz, M. G., Blumberg, P. M., Mischak, H., Mushinski, J. F., and Beaven, M. A. (1993) Ca(2+)-dependent and Ca(2+)-independent isozymes of protein kinase C mediate exocytosis in antigen-stimulated rat basophilic RBL-2H3 cells. Reconstitution of secretory responses with Ca2+ and purified isozymes in washed permeabilized cells. *J. Biol. Chem.* **268**, 1749–1756
8. Kawakami, T., Inagaki, N., Takei, M., Fukamachi, H., Coggeshall, K. M., Ishizaka, K., and Ishizaka, T. (1992) Tyrosine phosphorylation is required for mast cell activation by Fc epsilon RI cross-linking. *J. Immunol.* **148**, 3513–3519
9. Oliver, J. M., Burg, D. L., Wilson, B. S., McLaughlin, J. L., and Geahlen, R. L. (1994) Inhibition of mast cell Fc epsilon R1-mediated signaling and effector function by the Syk-selective inhibitor, piceatannol. *J. Biol. Chem.* **269**, 29697–29703
10. Nakanishi, S., Yano, H., and Matsuda, Y. (1995) Novel functions of phosphatidylinositol 3-kinase in terminally differentiated cells. *Cell Signal.* **7**, 545–557
11. Barker, S. A., Caldwell, K. K., Hall, A., Martinez, A. M., Pfeiffer, J. R., Oliver, J. M., and Wilson, B. S. (1995) Wortmannin blocks lipid and protein kinase activities associated with PI 3-kinase and inhibits a subset of responses induced by Fc epsilon R1 cross-linking. *Mol. Biol. Cell* **6**, 1145–1158
12. Barker, S. A., Lujan, D., and Wilson, B. S. (1999) Multiple roles for PI 3-kinase in the regulation of PLCgamma activity and Ca2+ mobilization in antigen-stimulated mast cells. *J. Leukoc. Biol.* **65**, 321–329
13. Kawakami, Y., Hartman, S. E., Holland, P. M., Cooper, J. A., and Kawakami, T. (1998) Multiple signaling pathways for the activation of JNK in mast cells: involvement of Bruton's tyrosine kinase, protein kinase C, and JNK kinases, SEK1 and MKK7. *J. Immunol.* **161**, 1795–1802
14. Ishizuka, T., Chayama, K., Takeda, K., Hamelmann, E., Terada, N., Keller, G. M., Johnson, G. L., and Gelfand, E. W. (1999) Mitogen-activated protein kinase activation through Fc epsilon receptor I and stem cell factor receptor is differentially regulated by phosphatidylinositol 3-kinase and calcineurin in mouse bone marrow-derived mast cells. *J. Immunol.* **162**, 2087–2094
15. Davis, R. J. (2000) Signal transduction by the JNK group of MAP kinases. *Cell* **103**, 239–252
16. Chang, L. and Karin, M. (2001) Mammalian MAP kinase signalling cascades. *Nature* **410**, 37–40
17. Manning, A. M. and Davis, R. J. (2003) Targeting JNK for therapeutic benefit: from junk to gold? *Nat. Rev. Drug Disc.* **2**, 554–565
18. Xu, R., Seger, R., and Pecht, I. (1999) Cutting edge: extracellular signal-regulated kinase activates syk: a new potential feedback regulation of Fc epsilon receptor signaling. *J. Immunol.* **163**, 1110–1114
19. Ishizuka, T., Terada, N., Gerwins, P., Hamelmann, E., Oshiba, A., Fanger, G. R., Johnson, G. L., and Gelfand, E. W. (1997) Mast cell tumor necrosis factor alpha production is regulated by MEK kinases. *Proc. Natl Acad. Sci. USA* **94**, 6358–6363
20. Zhang, C., Baumgartner, R. A., Yamada, K., and Beaven, M. A. (1997) Mitogen-activated protein (MAP) kinase regulates production of tumor necrosis factor-alpha and release of arachidonic acid in mast cells. Indications of communication between p38 and p42 MAP kinases. *J. Biol. Chem.* **272**, 13397–13402
21. Hirasawa, N., Sato, Y., Fujita, Y., and Ohuchi, K. (2000) Involvement of a phosphatidylinositol 3-kinase-p38 mitogen activated protein kinase pathway in antigen-induced IL-4 production in mast cells. *Biochem. Biophys. Acta* **1456**, 45–55
22. Sasaki, T., Wada, T., Kishimoto, H., Irie-Sasaki, J., Matsumoto, G., Goto, T., Yao, Z., Wakeham, A., Mak, T. W., Suzuki, A., Katada, T., Nishina, H., and Penninger, J. M. (2001) The stress kinase mitogen-activated protein kinase kinase (MKK)7 is a negative regulator of antigen receptor and growth factor receptor-induced proliferation in hematopoietic cells. *J. Exp. Med.* **194**, 757–768
23. Bennett, B. L., Sasaki, D. T., Murray, B. W., O'Leary, E. C., Sakata, S. T., Xu, W., Leisten, J. C., Motiwala, A., Pierce, S., Satoh, Y., Bhagwat, S. S., Manning, A. M., and Anderson, D. W. (2001) SP600125, an anthrapyrazolone inhibitor of Jun N-terminal kinase. *Proc. Natl Acad. Sci. USA* **98**, 13681–13686
24. Ura, S., Nishina, H., Gotoh, Y., and Katada, T. (2007) Activation of the c-Jun N-terminal kinase pathway by MST1 is essential and sufficient for the induction of chromatin condensation during apoptosis. *Mol. Cell Biol.* **27**, 5514–5522
25. Wada, T., Joza, N., Cheng, H. M., Sasaki, T., Kozieradzki, I., Bachmaier, K., Katada, T., Schreiber, M., Wagner, E. F., Nishina, H., and Penninger, J. M. (2004) MKK7 couples stress signalling to G2/M cell-cycle progression and cellular senescence. *Nat. Cell Biol.* **6**, 215–226
26. Kishimoto, H., Nakagawa, K., Watanabe, T., Kitagawa, D., Momose, H., Seo, J., Nishitai, G., Shimizu, N., Ohata, S., Tanemura, S., Asaka, S., Goto, T., Fukushi, H., Yoshida, H.,

Suzuki, A., Sasaki, T., Wada, T., Penninger, J. M., Nishina, H., and Katada, T. (2003) Different properties of SEK1 and MKK7 in dual phosphorylation of stress-induced activated protein kinase SAPK/JNK in embryonic stem cells. *J. Biol. Chem.* **278**, 16595–16601

27. Parravicini, V., Gadina, M., Kovarova, M., Odom, S., Gonzalez-Espinosa, C., Furumoto, Y., Saitoh, S., Samelson, L. E., O'Shea, J. J., and Rivera, J. (2002) Fyn kinase initiates complementary signals required for IgE-dependent mast cell degranulation. *Nat. Immunol.* **3**, 741–748
28. Momose, H., Kurosu, H., Tsujimoto, N., Kontani, K., Tsujita, K., Nishina, H., and Katada, T. (2003) Dual phosphorylation of phosphoinositide 3-kinase adaptor Grb2-associated binder 2 is responsible for superoxide formation synergistically stimulated by Fc gamma and formyl-methionyl-leucyl-phenylalanine receptors in differentiated THP-1 cells. *J. Immunol.* **171**, 4227–4234
29. Bain, J., McLauchlan, H., Elliott, M., and Cohen, P. (2003) The specificities of protein kinase inhibitors: an update. *Biochem. J.* **371**, 199–204

Biochemical and Biophysical Research Communications 390 (2009) 1129–1135

Contents lists available at ScienceDirect

Biochemical and Biophysical Research Communications

journal homepage: www.elsevier.com/locate/ybbrc

CrxOS maintains the self-renewal capacity of murine embryonic stem cells

Ryota Saito [a,b], Tokiwa Yamasaki [a,b], Yoko Nagai [a,b], Jinzhan Wu [a,b], Hiroaki Kajiho [b], Tadashi Yokoi [a,c], Eiichiro Noda [a,c], Sachiko Nishina [c], Hitoshi Niwa [d], Noriyuki Azuma [c], Toshiaki Katada [b], Hiroshi Nishina [a,*]

[a] Department of Developmental and Regenerative Biology, Medical Research Institute, Tokyo Medical and Dental University, Tokyo 113-8510, Japan
[b] Department of Physiological Chemistry, Graduate School of Pharmaceutical Sciences, University of Tokyo, Tokyo 113-0033, Japan
[c] Department of Ophthalmology, National Center for Child Health and Development, Tokyo 157-8535, Japan
[d] Laboratory for Pluripotent Cell Studies, RIKEN Center for Developmental Biology, Hyogo 650-0047, Japan

ARTICLE INFO

Article history:
Received 22 September 2009
Available online 1 October 2009

Keywords:
Embryonic stem cell
Self-renewal
In silico
Homeoprotein
CrxOS
foxD3

ABSTRACT

Embryonic stem (ES) cells maintain pluripotency by self-renewal. Several homeoproteins, including Oct3/4 and Nanog, are known to be key factors in maintaining the self-renewal capacity of ES cells. However, other genes required for the mechanisms underlying this process are still unclear. Here we report the identification by *in silico* analysis of a homeobox-containing gene, *CrxOS*, that is specifically expressed in murine ES cells and is essential for their self-renewal. ES cells mainly express the short isoform of endogenous CrxOS. Using a polyoma-based episomal expression system, we demonstrate that overexpression of the CrxOS short isoform is sufficient for maintaining the undifferentiated morphology of ES cells and stimulating their proliferation. Finally, using RNA interference, we show that CrxOS is essential for the self-renewal of ES cells, and provisionally identify *foxD3* as a downstream target gene of CrxOS. To our knowledge, ours is the first delineation of the physiological role of CrxOS in ES cells.

Introduction

Embryonic stem (ES) cells are pluripotent cells derived from the inner cell mass of preimplantation mammalian embryos. ES cells can be propagated stably in an undifferentiated state *in vitro* and, under the appropriate culture conditions, can be induced to differentiate into a variety of cell types. For example, forced transgenic expression of Pdx1 causes ES cells to differentiate into pancreatic cells (endoderm), whereas GATA2 expression promotes leukocyte differentiation (mesoderm), and Mash1 expression induces neuronal differentiation (ectoderm) [1,2]. This plasticity makes ES cell culture a useful tool for elucidating the functions of genes involved in early cellular differentiation.

Pluripotency and self-renewal are controlled by a transcriptional regulatory network that includes the transcription factors Oct3/4 and Nanog, both of which are encoded by genes that belong to the homeobox gene family [3,4]. However, other genes involved in ES cell pluripotency and self-renewal remain to be identified. Discovering these genes by conventional means is difficult, and the use of *in silico*-based strategies can significantly improve the chances of the detection of these genes. Data-mining and the automated tracking of new knowledge can greatly facilitate the creation of lists of genes potentially associated with a given process.

In this study, we performed comprehensive *in silico* analyses of the expression of a large collection of homeobox genes and have identified CrxOS [5] as a transcription factor expressed in pluripotent cells and tissues, including undifferentiated ES cells, blastocysts and adult testis. Furthermore, we have demonstrated a crucial physiological role for CrxOS in maintaining the self-renewal capacity of ES cells.

Materials and methods

In silico analyses of homeobox gene expression in ES cells and blastocysts. As our starting point, we used expression sequence tag (EST) clusters of 240 murine genes containing a homeobox that were registered in NCBI's organized view of the transcriptome (Unigene; http://www.ncbi.nlm.nih.gov/unigene/). We then calculated the numbers of EST clones of the above 240 genes in the NCBI/Unigene/DDD (Digital Differential Display; http://www.ncbi.nlm.nih.gov/UniGene/ddd.cgi?TAX=9913) and NCBI/Unigene/dbEST (http://www.ncbi.nlm.nih.gov/dbEST/index.html) datasets.

ES cell culture. The murine ES cell lines E14K and MG1.19 were grown as previously described with slight modifications [6–8]. Briefly, both ES cell lines were routinely cultured in gelatin-coated dishes in Dulbecco's modified Eagle's medium (high glucose; Invitrogen) supplemented with 15% fetal bovine serum, 1000 U/mL leukemia inhibitory factor (LIF), and 0.1% 2-mercaptoethanol. Cells

* Corresponding author. Address: Department of Developmental and Regenerative Biology, Medical Research Institute, Tokyo Medical and Dental University, Tokyo, 1-5-45 Yushima, Bunkyo-ku, Tokyo 113-8510, Japan. Fax: +81 3 5803 5829.
E-mail address: nishina.dbio@mri.tmd.ac.jp (H. Nishina).

0006-291X/$ - see front matter © 2009 Published by Elsevier Inc.
doi:10.1016/j.bbrc.2009.09.118

were passaged every 2–3 days. Embryoid bodies (EB) were derived from E14K ES cells by three-dimensional culture for 6 days in the absence of LIF. For transfection experiments, MG1.19 ES cells were cultured in the presence of 500 μg/mL G418 (Sigma) and 2 μg/mL puromycin (Sigma). Viable cell counts were performed by staining the cells with trypan blue dye and counting them on a hemocytometer. A cell-counting kit (WST-8; Dojin) was also used according to the manufacturer's protocol. Statistical analyses were performed using the paired two-tailed Student's *t* test or Welch's test using R.

Fluorescence-activated cell sorter (FACS) analysis. Single-cell suspensions of ES cells were stained with propidium iodide (PI) and analyzed using a FACSCalibur (Becton Dickinson Biosciences).

RNA isolation and RT-PCR analysis. Total RNAs were prepared with TRIzol reagent (Invitrogen), and cDNAs were prepared from total RNA using SuperScript (Invitrogen) and random primers according to the manufacturer's instructions. For PCR amplification of cDNAs, the following gene-specific primers were used:

β-actin-forward (F), CATCACTATTGGCAACGAGC;
β-actin-reverse (R), CGCAGCTCAGTAACAGTCC;
CrxOS-F (1), GTTTGAATCCTAAATCCTTAGAGC;
CrxOS-F (2), CTCCTGTACCCTGGGTCCCCTTG;
CrxOS-R, GTACCTCTTCTCCTTCCCACAAA;
ef1α-F, TCACACAGCCCACATAGCAT;
ef1α-R, CACCACTGATTAAGACTGGG;
foxD3-F, TGACCCCGAACAAGCCCAAGAACA;
foxD3-R, AGGCTCCGAAGCTCTGCATCATCA;
hprt-F, GAGATGGGAGGCCATCACATTGTG;
hprt-R, GGCCTGTATCCAACACTTCGAGAG;
nanog-F, AGGGTCTGCTACTGAGATGCTCTG;
nanog-R, CAACCACTGGTTTTTCTGCCACCG;
oct-3/4-F, CTGAGGGCCAGGCAGGAGCACGAG;
oct-3/4-R, CTGTAGGGAGGGCTTCGGGCACTT;

Preparation of anti-CrxOS antibody and Western blot analysis. A polyclonal anti-CrxOS antibody preparation (pAb) was generated by immunizing rabbits with CrxOS peptide conjugated with keyhole limpet hemocyanin and cysteine (KLH-C-QSALDGTSSPSHKA; Sigma). The anti-CrxOS pAb was used in experiments at a dilution of 1:200. For Western blots, ES cells were lysed with RIPA buffer [10 mM Tris–HCl (pH 7.4), 1 mM EDTA, 150 mM NaCl, 1% NP-40, 0.1% (w/v) sodium deoxycholate, 0.1% (w/v) SDS, 5 μg/mL aprotinin] and the supernatants were boiled with Laemmli sample buffer. Lysates were subjected to SDS–PAGE followed by immunoblotting with anti-CrxSO pAb, anti-c-Myc antibody (clone 9E10, Sigma), or anti-GAPDH antibody (clone 6C5, Santa Cruz).

Vector construction, transfection, and puromysin selection. The pPyCAGIP episomal expression vector [8] was used to make constructs containing the human histone H1 promoter and shRNA sequences as follows:

CrxOS shRNA: 5′-GATCCCCAGATTATGGTCACTAGACTGAAACTGAAATTCAAGAGATTTCAGTTTCAGTCTGGTGGCCATGATCTTTTTTGGAAA-3′; *Control* (*EGFP*) shRNA: 5′-GATCCCCGCAGCACAACTTCTCCAAGTCCACCATGCTTCAAGAGAGCATGGCGGACTTGAAGAAGTCGTGCTGCTTTTTGGAAA-3′. shRNAs were designed as described previously [9] with a slight modification. Briefly, a DNA fragment containing a Kozak sequence, a Myc tag sequence, and a multi-cloning site was inserted into EcoRI-digested pPyCAGIP to give the pPyCAGmycIP episomal expression vector [10]. For CrxOS overexpression vectors, the cDNAs encoding the long and short isoforms of CrxOS (Supplementary Fig. 1A) were obtained from E14K ES cells by PCR amplification and inserted into pPyCAGmycIP.

The RNAi-insensitive *CrxOS short* mutant was generated by introducing three silent mutations into the shRNA target sequence in *CrxOS short* such that "agatcatggcCaccagActgaaActgaaa" was converted to "agatcatggcTaccagGctgaaGctgaaa". Transfection into MG1.19 ES cells was performed with LipofectAMINE 2000 (Invitrogen) according to the manufacturer's protocol with a slight modification. Puromycin selection (2 μg/ml) was performed at 24 h post-transfection.

Results

Identification of the homeobox gene CrxOS as an ES cell-specific gene by in silico analysis

To identify ES cell-specific homeobox genes, we searched for ESTs among 240 murine genes known to contain a homeobox and registered in the NCBI EST database. We performed an *in silico* analysis of these genes by determining their levels of expression in ES cell and blastocyst cDNA libraries. We anticipated that ESTs associated with ES cell-specific homeobox genes would occur at a higher ratio in ES cells and blastocysts than would most other ESTs. After calculating EST frequencies for all 240 homeobox genes, we found that the top ten most frequent genes in ES cells and blastocysts were *CrxOS* [5], *nanog* [3], *sebox* [11], *oct3/4* [4], *gpbox* [12], Mm.158735, *pitx3* [13], Mm.201536, and *gbx-2* [14] (Supplementary Table 1). The proteins encoded by the *nanog* and *oct3/4* genes are well-known pluripotency-associated transcription factors that are crucial for stable *in vitro* propagation of ES cells in an undifferentiated state. In contrast, although *CrxOS* has been described as a homeobox gene expressed in murine retina [4], its expression and function during murine development are unknown.

CrxOS mRNA is specifically expressed in undifferentiated ES cells, blastocysts and adult testis

To examine the expression of *CrxOS* mRNA in various tissues, we performed RT-PCR and Northern analyses. *CrxOS* mRNA was expressed in undifferentiated ES cells but not in ES cells induced to differentiate by removal of LIF from the culture medium (Fig. 1A and Supplementary Fig. 1B). Furthermore, *CrxOS* mRNA

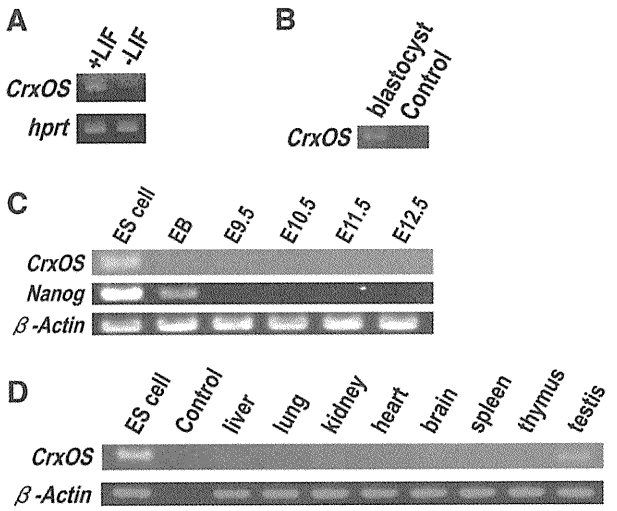

Fig. 1. Expression profiles of *CrxOS* mRNA in murine cells and tissues. (A) Dependence on LIF. E14K ES cells were cultured in the presence or absence of LIF, and levels of *CrxOS* mRNA were assessed by RT-PCR. (B, C, and D) *CrxOS* mRNA expression in mouse tissues as determined by RT-PCR. (B) Blastocysts. (C) E14K ES cells (LIF+), embryoid bodies (EB), and E9.5–E12.5 murine embryos as indicated. Nanog, positive control. β-Actin, loading control. (D) Adult murine tissues as indicated, with ES cells assessed as a positive control. Control, no reverse transcriptase.